Pacific Community
Communauté du Pacifique

Nauru
Coastal risk assessment

Moritz Wandres, Judith Giblin, Antonio Espejo, Tomasi Sovea, Russell Simpson, Naomi Jackson, Azaria C. Pickering, and Herve Damlamian

Nauru
Coastal risk assessment

Moritz Wandres, Judith Giblin, Antonio Espejo, Tomasi Sovea,
Russell Simpson, Naomi Jackson, Azaria C. Pickering, and Herve Damlamian

Geoscience, Energy and Maritime Division of the Pacific Community

Pacific Community
Communauté du Pacifique

Suva, Fiji, 2023

Original text: English

Pacific Community Cataloguing-in-publication data

Wandres, Moritz
Nauru coastal risk assessment / written by Moritz Wandres, Judith Giblin, Antonio Espejo, Tomasi Sovea, Russell Simpson, Naomi Jackson, Azaria C. Pickering, and Herve Damlamian

1. Risk assessment — Nauru.
2. Coastal zone management — Risk assessment — Nauru.
3. Climatic changes — Risk assessment— Nauru.
4. Climatic changes — Management — Nauru.
5. Climatic changes — Nauru.
6. Coastal zone management — Nauru.

I. Wandres, Moritz II. Giblin, Judith III. Espejo, Antonio IV. Sovea, Tomasi V. Simpson, Russel VI. Jackson, Naomi VII. Pickering, Azaria C. VIII. Damlamian, Herve IX. Title X. Pacific Community

577.51099685 AACR2

ISBN: 978-982-00-1489-3

Photo credit: Pacific R2R Ridge to Reef Programme

Prepared for publication at SPC's Suva Regional Office,
Private Mail Bag, Suva, Fiji, 2023
www.spc.int | spc@spc.int

Contents

Abbreviations

AMBUR – Analysing Moving Boundaries Using R

ARI – Annual recurrence interval

CAWCR – Centre for Australian Weather and Climate Research

DEM Digital elevation model

ENSO – El Niño Southern Oscillation

η_2 – 2% exceedance water level nearshore

η_{MSLA} – Mean sea-level anomalies

η_{tide} – Tide level

EEZ – Exclusive economic zone

GFDRR – Global Facility for Disaster Reduction and Recovery

GMSL – Global mean sea level

H_b – Breaker wave height

H_s – Significant wave height

IG – Infragravity

IPCC AR6 – Intergovernmental Panel on Climate Change Sixth Assessment Report

MJO – Madden-Julian Oscillation

MSL – Mean sea-level

OSM – Open Street Map

PCRAFI – Pacific Catastrophe Risk Assessment & Financing Initiative

PacRIS – Pacific Risk and Information Systems Database

QGIS – Quantum Geographic Information System

SSP – Shared socioeconomic pathway

SOPAC – South Pacific Commission

θ_p – Peak wave direction

T_p – Peak wave period

SLR – Sea-level rise

TWL – Total water level

WLR – Weighted linear regression

Figures and tables

Executive summary

Most of Nauru's developments and assets are located in low-lying areas that are exposed to wave-driven inundation and erosion. The frequency and impact of these inundation events is expected to increase in the coming decades due to sea-level rise. In the present study we combine numerical and empirical models to investigate coastal inundation risk by considering tides, sea-level anomalies, waves and sea-level rise. We further explore Nauru's shoreline change between 1992 and 2020. With the open-source risk modelling software RiskScape, we investigate the exposure of assets and population to inundation. The impact of climate change is assessed by applying sea-level rise projections from the shared socioeconomic pathways (SSPs) SSP1-1.9 and SSP5-8.5 for two time horizons (2050 and 2100).

Under present sea-level conditions, a 5-year annual recurrence interval (ARI) inundation event floods 6.2% of Nauru's buildings and 2.7 km of roads. Results indicate that sea-level rise will clearly exacerbate the risk of coastal flooding, with 16.7% of buildings and 8.1 km of roads inundated by a 5-year ARI event by 2100 (under the SSP5-8.5 scenario). The annual expected loss from coastal flooding for all of Nauru based on the present-day sea level is estimated to be roughly USD 1.3 million/year. This amount is expected to increase between 3.3 to 5.7 times by 2100.

While a clear link between sea levels and hazard exposure was found, the impact of climate change on the shoreline remains less clear. Major changes of the shoreline over recent decades have mainly been attributed to anthropogenic interventions, and further research is needed to link climate drivers to erosion and accretion.

A detailed breakdown of shoreline change, hazard exposure, damage, and loss is provided in this report. The information and maps produced will enable decision makers to prioritise funding, mitigation strategies and future research.

1. Introduction

Over the last century, widespread damage during the Second World War, monocultural farming of coconut palms, and decades of open-cast phosphate mining have led to the destruction and degradation of Nauru's interior endemic flora and fauna (Thaman 1992). The destruction of the island's interior has also hindered economic and humanitarian development (Pollock 2014). Most of the country's developments and assets are in low-lying areas along the coastline, exposing them to damage from shoreline change and wave-driven inundation. Recent mapping of the country's freshwater reserve also revealed that many of Nauru's aquifers are located close to the coastline (Alberti et al. 2017). Coastal inundation has therefore been identified as one of Nauru's major threats, particularly under the premise of climate change and associated increased sea levels (e.g., Allis et al. 2020; Maharaj 2000).

Coastal inundation is a compound event where waves, tides, and sea-level anomalies all interact to create an extreme total water level (TWL) nearshore and flood the coastal areas. On reef-fronted islands, the wave contribution to TWL nearshore consists of wave setup (e.g., Becker et al. 2014) and infragravity (IG) waves (e.g., Baldock 2012; Pomeroy et al. 2012). Extreme waves causing inundation in the tropical Pacific have been shown to be generated by distant extra-tropical storms (e.g., Hoeke et al. 2013; Wandres et al. 2020), distant tropical cyclones (e.g., Hoeke et al. 2021), and local tropical cyclones (e.g., Terry & Lau 2018).

A recent report by Allis et al. (2020) investigates the risk of Nauru's coastal areas due to coastal flooding using a "bathtub" approach to estimate flooded areas. In the study, the authors establish thresholds for extremely high tides (king tides) and investigate the risk to population and infrastructure under different sea-level rise projections. While the study serves as a first approximation at establishing the risk of coastal flooding, it omits wave contribution to TWL. Regardless, the study echoes the sentiment of a previous investigation (Maharaj 2000) that the risk exposure of coastal infrastructure will increase with rising sea levels.

Extensive adaptation measures are needed to increase the resilience of existing infrastructure against coastal flooding and climate change. However, most engineering solutions come at a high cost. While land rehabilitation of Nauru's interior has been ongoing to enable the relocation of assets from low-lying areas, there are doubts that the current rate of rehabilitation will be sufficient to accommodate sea-level rise (Allis et al. 2020). At the same time, foreshore developments continue, often with little consideration for the risk of these developments to surrounding areas (Maharaj 2000). Critical infrastructure, including the power station, roads, schools, and hospitals, are located in low-lying coastal areas that are susceptible to coastal inundation (Republic of Nauru 2014). A thorough understanding of the risk to Nauru's low-lying areas should therefore be a priority to inform adequate coastal development.

The aim of this study is to identify and assess the risk of Nauru's population and infrastructure to coastal flooding to help decision-makers prioritize funding and target their resources. We distinguish between climate change-related risk and anthropogenic causes of elevated risk. The report is structured as follows: Chapter 2 provides background information on Nauru's climate and climate change projections. Chapter 3 describes the methodologies used to investigate inundation, shoreline change, asset changes, and the risk assessment. In chapter 4 we present the results, which are then discussed in chapter 5.

2. Background

Nauru is a single, oval-shaped, raised limestone island located approximately 40 km south of the equator (Figure 2.1). The total land area is 21 km^2, with an exclusive economic zone (EEZ) of 308,480 km^2. The island is divided into two plateau areas. The lower part, known as "Bottomside", is a few metres above sea level. The top part, known as "Topside", is typically < 30 m above mean sea level. Topside features pinnacles and outcrops of limestone which were mined for high-grade phosphate rock. The lower narrow coastal plane is 150–300 m wide and surrounded by coral reef. The maximum height of the island above sea level is 71 m (Republic of Nauru 2014). Nauru has a population of 11,690 people, with 93% of the population living within 1 km from the coast (Andrew et al. 2019).

Figure 2.1: Map of Nauru

2.1. Nauru's climate

Nauru has consistently warm monthly average temperatures throughout the year, with a wet season from November to April, and drier conditions from May to October. The wet season is affected by the movement of the Intertropical Convergence Zone and the South Pacific Convergence Zone. The main driver of climate variability is the El Niño Southern Oscillation (ENSO). El Niño events tend to bring warmer, wetter conditions than normal and higher rainfall, with approximately 4500 mm of annual rainfall. During La Niña events, the onset of the wet season is delayed, providing drier than normal conditions and resulting in extended drought, with approximately 500 mm of annual rainfall. Nauru can also be affected by the West Pacific Monsoon as the persistent monsoon westerly winds reach far east. The West Pacific Monsoon phase and strength varies and is usually associated with strong El Niño events (Australian Bureau of Meteorology and CSIRO 2014; Republic of Nauru 2014). In addition, the Madden-Julian Oscillation (MJO), an eastward moving system of clouds and rainfall near the equator that develops in the western Indian Ocean and moves eastward to the western Pacific Ocean, typically recurs every

30 to 60 days. The MJO brings significant variations in convection and is one of the reasons for intra-seasonal rainfall variability in the tropics. Mostly active in December–February, it often results in short wet and dry periods within a single monsoon season (CSIRO et al. 2015).

Coastal flooding can cause erosion, destruction of infrastructure, contamination of freshwater reserves and even loss of lives (Hoeke et al. 2013; Smith and Juria 2019; Storlazzi et al. 2018). The hazard of coastal flooding in Nauru has been identified as high by the World Bank Global Facility for Disaster Reduction and Recovery (GFDRR; Fraser et al. 2017). The methodology to determine flood hazard in the GFDRR study was based on Muis et al. (2016), who used a global tide and a global storm surge model to estimate extreme water levels globally. This method did not include the contribution of waves to extreme water levels. While Nauru is close to the equator and therefore has had no recorded tropical cyclones since the 1970s, it can still be exposed to swells generated by distant tropical and extratropical storms (e.g., Hoeke et al. 2013; Hoeke et al. 2021; Wandres et al. 2020).

The wave climate in Nauru is dominated by the easterly trade winds that generate short period waves from the east. According to Bosserelle et al. (2015), who analysed the wave climate of most countries in the South Pacific using a long-term wave hindcast, Nauru has an annual mean wave height of 1.3 m with a mean wave period of 10 s from 80°. Wave conditions follow a seasonal cycle with the largest waves occurring during the boreal winter between December and March. At the same time, a shift in wave direction can be observed with north-easterly wave directions during the boreal winter and south-easterly wave directions during the austral winter (Figure 2.2; Australian Bureau of Meteorology and CSIRO 2014). This shift is likely linked to the seasonal north-southward oscillation of the Intertropical Convergence Zone.

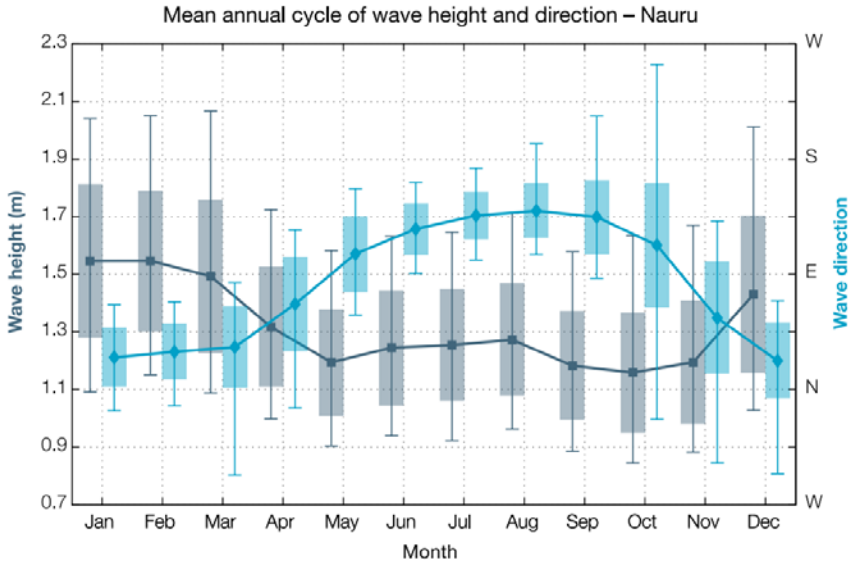

Figure 2.2: Wave height (grey) and wave direction (blue) seasonality in Nauru from 1979–2009. Shaded boxes represent one standard deviation around the monthly means, and error bars indicate the 5–95% range of year-to-year variability in wave climate. The wave direction shows the direction the wave is travelling from (not the direction they are travelling towards) (Australian Bureau of Meteorology and CSIRO, 2014).

In the analysis by Bosserelle et al. (2015), different ARIs of significant wave heights were provided (Table 1). The report highlights that while the average wave climate is dominated by waves from the east (i.e., waves generated by the predominant trade winds), most large wave events (i.e., wave heights > 2 m) come from a westerly direction. In fact, the top five largest wave events in the period analysed by Bosserelle et al. (2015) approached Nauru from the west because of tropical depressions and tropical cyclones in the South Pacific. Due to the well documented increase in tropical cyclone activity in the western South Pacific during positive phases of ENSO (e.g., Chand et al. 2013; Chand and Walsh 2009), it is unsurprising that four of the five largest wave events occurred during El Niño years (Table 2.2).

	Bosserelle (2015)
Largest wave height (90th Percentile)	1.68 m
Severe wave height (99th Percentile)	2.12 m
1-year ARI wave height	2.40 m
10-year ARI wave height	3.33 m
20-year ARI wave height	3.71 m
50-year ARI wave height	4.32 m
100-year ARI wave height	4.87 m

Table 2.1: Extreme wave height summary for Nauru (Bosserelle et al. 2015).

Rank	Date	Height (m)	Period (s)	Direction (°)
1	29/03/1980	4.28	10	275
2	05/01/1992	3.77	10	274
3	30/11/2002	3.42	9	264
4	18/12/1994	3.14	10	266
5	14/02/1990	3.11	8	289

Table 2.2: Nauru's five largest wave events (Bosserelle et al. 2015).

ENSO also influences sea-level anomalies, with the top 10 highest mean sea-level anomaly events occurring during El Niño or ENSO-neutral years (Figure 2.3). The interannual variability of the mean sea level is around 23 cm after removal of the seasonal cycle (Australian Bureau of Meteorology and CSIRO 2011). Seasonally, the mean sea level varies with highest water levels between November and March due to the earth's proximity to the sun and the resulting spring tides during these months. Allis et al. (2020) define the "king tide" elevation in Nauru as the 1% exceedance probability at the present-day sea level. The true 1% tide gauge record elevation was rounded to 2.7 m (above Nauru Island Datum or 1.27 m above 1993–2020 mean sea level), which equates to a 0.72% exceedance probability. By this definition, about five tides per year are higher than the "king tide".

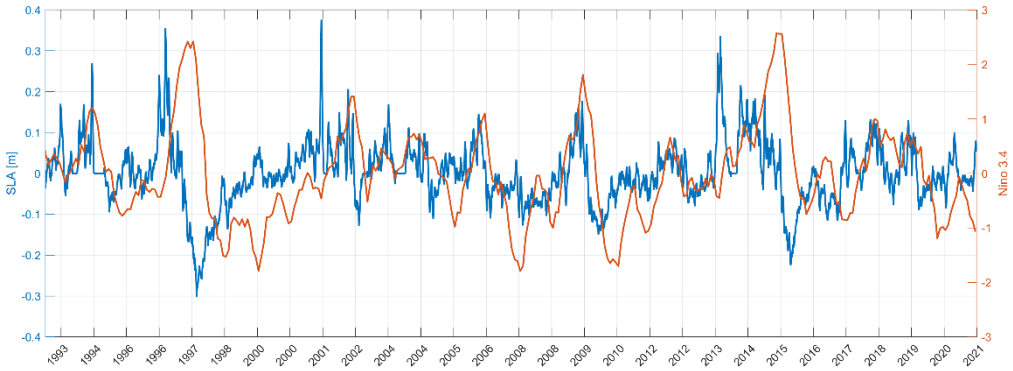

Figure 2.3: Sea-level anomaly (blue line) for Nauru and ENSO phase (orange line).

2.2. Climate change projections

An analysis of tide gauge data by Allis et al. (2020) shows that Nauru's monthly maximum sea level has increased at a relative rate of 5.7 mm per year (not accounting for vertical land motion) between 1993 and 2019 (5.4 mm/year was obtained in the analysis performed in this study). The future rise in global mean sea level (GMSL) is dependent on humanity's ability (or lack thereof) to reduce greenhouse gas emissions. The Intergovernmental Panel on Climate Change Sixth Assessment Report (IPCC AR6) uses five different shared socioeconomic pathways (SSPs) to assess the range of potential climate change scenarios. It is projected that the global mean sea level will rise between 0.18 m (0.15–0.23 m, SSP1-1.9) and 0.23 (0.20–0.30 m, SSP5-8.5) by 2050 and between 0.38 m (0.28–0.55 m, SSP1-1.9) and 0.77 m (0.63–1.02 m, SSP5-8.5) by 2100, relative to the 1995–2014 mean sea level (IPCC 2021).

IPCC AR6 also states that there is high confidence that the occurrence and magnitude of compound flooding in coastal regions will increase in the future due to sea-level rise. Additionally, the frequency of intense tropical cyclones is projected to increase.

2.3. Coastal erosion

Shoreline erosion is the loss of coastal lands due to natural or human induced practices. Several studies have presented evidence that coral growth rates have been able to keep up with sea-level rise in the tropical Pacific over recent decades (e.g., Beetham et al. 2017; Tuck et al. 2019; Webb and Kench 2010). Other studies, however, have suggested that rates of sea-level rise will be greater than reef accretion rates due to an overall degradation of reef health over the coming decades (Perry et al. 2018). Detailed case studies are therefore necessary to understand the interaction of sea-level rise, changes in storm intensity and frequency, and coral health and shoreline change (e.g., Beetham and Kench 2018; Hoeke et al. 2021).

In 2000, a field reconnaissance survey by the South Pacific Commission (SOPAC) was conducted to examine Nauru's coast and identify areas of coastal erosion. The survey revealed severe erosion on the shoreline adjacent to Anibare harbour, the airport runway extension in Yaren, near the Gabab Channel resulting from sand mining, and from seawall around the whole island (He 2000). For locations, refer to Figure 2.1. While these changes can likely be attributed to human interaction, it is unclear how human development and/or climate change have impacted Nauru's shoreline since this analysis was undertaken.

3. Methodology

3.1. Coastal hazard assessment

A preliminary coastal inundation risk assessment considering tides, mean sea-level variability and wave contribution (wave runup/setup) to the total water level (TWL) was undertaken to evaluate potential risk to property, infrastructure and coastal communities in Nauru. Coastal inundation risk was assessed for 5-, 10-, 25-, 50- and 100-year ARIs. Sea-level rise projections of the shared socioeconomic pathways (SSPs) SSP1-2.6 and SSP5-8.5 H+ were applied to inform coastal adaptation planning. The methodology is composed of six steps, which are briefly described below.

Data: Infrastructure, tide, wave, elevation, and sea-level rise projection data were obtained from various freely available sources. The data sources are provided in Table 3.1.

Information	Source
Infrastructure	• GIS polygon data for buildings, roads, airport, population, land, tanks and poles sourced from SPC
Tide	• Nauru tide gauge record from the Pacific Sea Level and Geodetic Monitoring Project (Geoscience Australia and SPC)
Waves	• CAWCR Wave Hindcast, 4 km Pacific grid (CSIRO, Durrant et al. [2014])
Elevation	• 1-m resolution LiDAR survey collected in 2014 (NID vertical datum)
Sea-level rise	• AR6 regional mean sea-level rise including vertical land movement from Table 3.9 in https://www.theprif.org/sites/default/files/documents/PRIF_SLR-Report_Digital_0.pdf

Table 3.3: Data sources

Tide gauge analysis: To provide information on the individual components of sea level, Nauru's tide gauge, located in Aiwo (00° 31′ 55″ S, 166° 54′ 33″ E), was used to derive tides and mean sea-level anomalies (η_{MSLA}).

Wave contribution to TWL: Extreme sea levels include contribution from tides, mean sea-level anomaly, storm surge and wave setup/runup. Tide gauge records generally neglect the wave contribution to TWLs as the gauges are usually installed in wave-sheltered areas. For this initial assessment, the effect of wave setup (including infragravity waves) was estimated based on the empirical formula of Merrifield et al. (2014), which provides the 2% exceedance water level (η_2) near the shore from breaking wave heights at the outer reef.

$$\eta_2 = b_1 H_b + b_0 \quad (1)$$

Where is the breaker wave height, is the offshore significant wave height, is the offshore peak period, and is the offshore peak direction:

$$H_b = \left(H_s^2 T_p (4\pi)^{-1} - \cos(\theta_p - \theta_N)\sqrt{\gamma g}\right)^{\frac{2}{5}} \quad (2)$$

Following Hoeke et al. (2021), who studied wave-driven flooding in Tuvalu and Kiribati triggered by distant Tropical Cyclone Pam, we assumed the two empirical coefficients to be $b_1 = 0.3$ and $b_0 = -0.1$. γ is the ratio of breaking H_b to breaking water depth, which we assumed to be 1 in line with Becker at al. (2014) and Vetter et al. (2010). θ_N is the local shore-normal angle.

Although this formula was obtained from observations on Majuro and Roi-Namur atolls in Marshall Islands, due to the similarities in reef morphology (reef flat width and depths) and frictional roughness, it has been applied to Nauru, similar to previous work by Hoeke et al. (2021). Breaking wave heights were determined based on the

closest Centre for Australian Weather and Climate Research (CAWCR) hindcast point (see wave rose in Figure 3.1) and considering the orientation of evenly 100-m spaced profiles along Nauru's coastline (Figure 3.1).

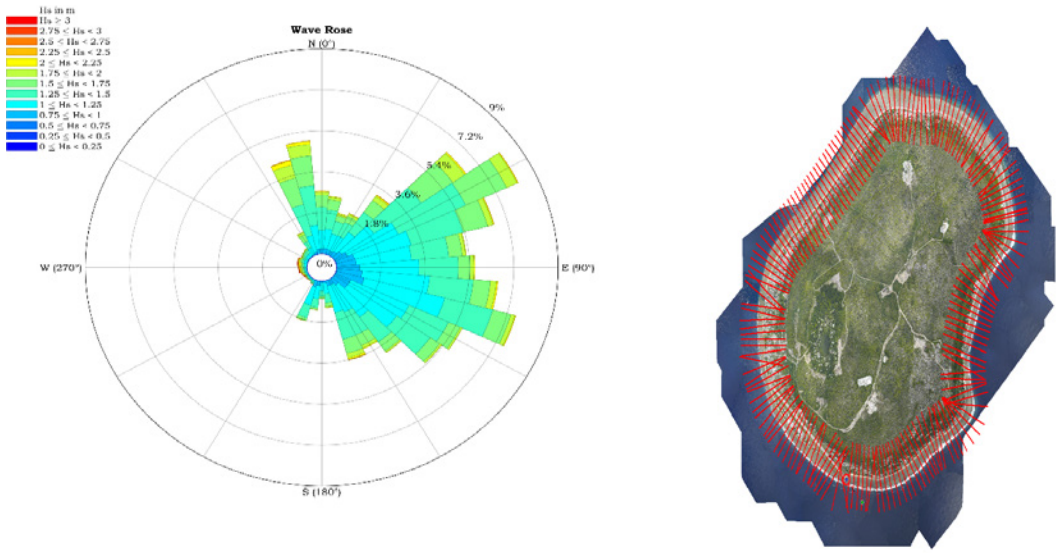

Figure 3.1: (left) Wave rose at 166.92°E, 0.5°S from CAWCR hindcast. (right) Profiles defining coastal orientation along Nauru.

TWLs and extreme value distributions: Once the wave contribution was assesed spatially along Nauru's coastline, TWLs were reconstructed as the linear summation of sea-level anomaly (η_{MSLA}), tide (η_{tide}) components:

$$TWL = \eta_{MSLA} + \eta_{tide} + \eta_{StormSurge} + \eta_2 \quad (3)$$

In total, 28 years of hourly TWL data were obtained, enough to confidently fit extreme value distribution of TWL and evaluate inudation hazard up to 500 years ARI. Here, a generalized extreme value (GEV) distribution was fitted to the annual maxima of TWL determined at every point.

Sea-level rise (SLR) projections: Nauru's local SLR projections for the low emissions scenario (SSP1-2.6) and very high emissions (SSP5-8.5 H+) scenario, and for the years 2050 and 2100 were considered to assess the range of plausible events, from the lower to the upper bound. SLR values in Table 3.2 were added to the different ARIs obtained for the present mean sea level.

SSP	2050	2100
SSP1-2.6	0.26 m	0.61 m
SSP5-8.5 H+	0.31 m	1.07 m

Table 3.4: SLR projections considered in this study.

Hazard risk mapping: Based on the TWLs estimated along Nauru's coastline for the different SLR scenarios and ARIs, a quadratic surface was fitted to account for associated TWL variability related to different wave exposures. These surfaces were intersected ("bathtub" approach) with the 5-m resolution digital elevation model (DEM) of Nauru derived from a national-scale light detection and ranging (LiDAR) survey.

3.2. Asset change analysis

To link historic extreme water levels to impact and risk, and to split climate related events from anthropogenic interventions, an asset change analysis was undertaken. The asset change analysis focused on three major assets along the coastline: buildings, seawall development and population.

Building data collected from Pacific Risk and Information Systems Database (PacRIS) 2012 and 2020 building data (WorldView-2 and OpenStreetMap [OSM]) were compared to determine developments that had taken place in each district.

Seawall data were extracted from the 2014 LiDAR survey and 2020 WorldView-2 image. Seawall lengths were derived for the two years and the change over time was calculated for each district.

A study of population trends between 1992 and 2019 was conducted. Population data were collected for 1992, 2002, 2011 and 2019. Percentage growth between each time slice and between 1992 and 2019 was calculated to determine the population trend for Nauru.

3.3. Shoreline change analysis

Sandy shorelines are dynamic, naturally changing shape and position over multiple temporal and spatial scales as they respond to ocean forcings (e.g., Burningham and Fernandez-Nunez 2020). Waves are the primary driver of longshore sediment transport. While the overall wave regime in Nauru is quite variable (Bosserelle et al. 2015), the sediment distribution around Nauru's coastline is dominated by waves generated by the easterly trade winds. Finer sands are deposited on the western coastline (leeward of the dominant trade winds), while coarser sand and coral rubble are deposited on the eastern coastline, which is dominated by the short period wave action generated by the trade winds (He 2000). As ocean forcings vary over seasonal, inter-annual and decadal scales, shorelines adapt. Additionally, shoreline change can also be episodic, with abrupt changes driven by large swell events, storms and tropical cyclones (He 2000). Longer term, Nauru has been experiencing relative sea-level rise rates higher than the global average, which threatens coastal livelihoods and infrastructure (The World Bank Group 2021) and may affect shoreline change over the coming decades.

Over recent years, global shorelines have also been significantly affected by local anthropogenic activities due to urbanisation, sand mining, nearshore dredging operation and inadequate coastal engineering solutions.

Mapping past shoreline changes and understanding the causes and local responses are important steps towards strengthening risk knowledge and supporting risk-informed investment within the coastal zone and long-term development strategies in small island nations. With sea-level rise expected to increase wave power at the shore and ocean acidification potentially leading to a reduced long-term sand supply, increasing our understanding of changing shorelines is critical to the development of efficient climate change adaptation solutions for Nauru.

The methodology used in this study is threefold:

1. Image processing
2. Shoreline extraction
3. Analysis

A schematic overview of the workflow is provided in Figure 3.2.

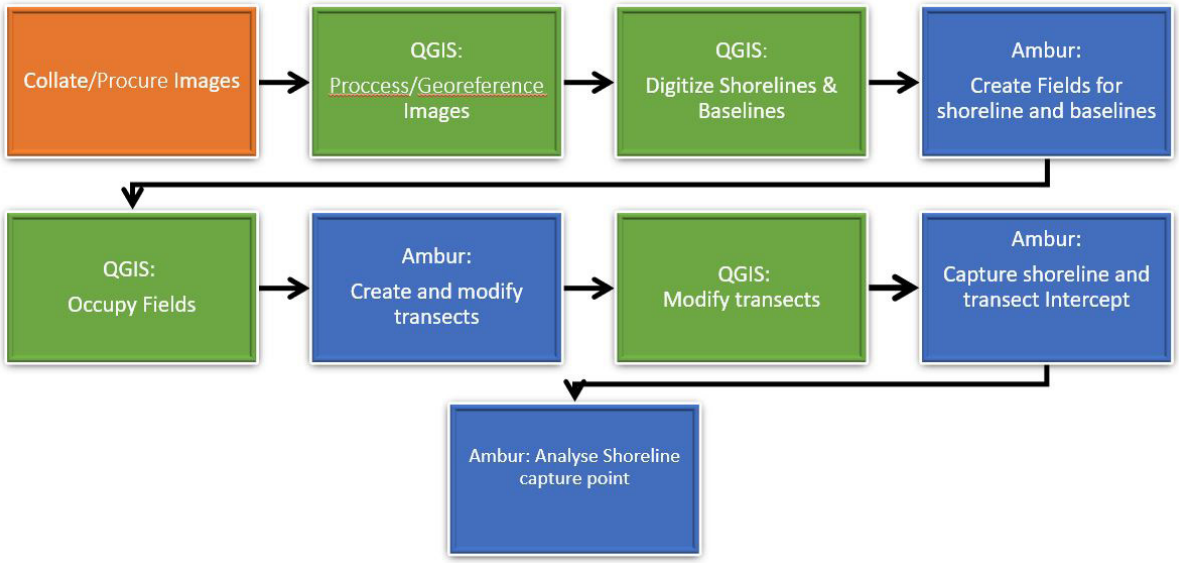

Figure 3.2: The flow of work that was undertaken during this study. The orange box indicates the collation of images and does not require any special software, the green boxes highlight processes conducted using QGIS and the blue boxes show process conducted using AMBUR (Jackson et al. 2012).

3.3.1. Image collation

A total of six images were used to extract shoreline data. The imagery collected came from an aerial image in 1992, satellite from Quick Bird dated 2005, World View for 2018 and 2020, and LiDAR data from 2010 and 2014.

3.3.2. Image pre-processing

… Specific contrast enhancement

This step consists of adjusting the brightness and the contrast of the pansharpened images to enhance some of the features in order to delineate the shoreline proxies more efficiently and accurately.

… Geometric correction

Georectification was conducted to ensure that all images were overlayed correctly to reduce errors in shoreline extraction. The LiDAR data for 2014 was used as a reference against which all other datasets were corrected using various ground control points, such as buildings, coral heads, and special landmarks spread across the images.

3.3.3. Digitizing

Digitizing is a process of converting geographic data from satellite images, aerial images, scanned images or maps into vector data by tracing the features. The available images were digitized at a scale view of 1:500 in Quantum Geographic Information System (QGIS). The shoreline was digitized manually, with instantaneous watermark used as the definition of shoreline in this study.

3.3.4. R-Studio data analysis

After extracting the historical shorelines for each of the shoreline proxies, the open-source package in R software AMBUR (Analysing Moving Boundaries Using R) (Jackson et al. 2012) was used to run a historical shoreline change analysis. The package allows the import of shoreline data in ESRI shapefile format. After defining transects across the study site, the software then captures the intersection of each shoreline along these transects and performs the analysis. In this study, transects were constructed in AMBUR at 50-metre intervals. Outputs from the analyses include data tables, graphics, and geospatial data, which are useful in rapidly assessing trends and potential errors in the dataset.

The output data from AMBUR (i.e., shoreline positions along each transect) were then further refined.

In this study, the uncertainty was quantified by evaluating three sources of error:

- Pixel error relates to image precision and is taken from the resolution of the imagery (pixel size).
- Georectification error aims to quantify the amount of positional error produced during geometric correction. It is calculated as the root mean square error between the control points on the reference image (i.e., LiDAR) against the georeferenced image.
- Digitizing error is the error introduced by manually digitizing the shoreline. In this study, digitizing error was quantified for each shoreline dataset by repeatedly (10 times) digitizing a subset of the shoreline (500 m) and measuring the maximum positional error.

Following Genz et al. (2007), the total uncertainty is calculated using the following equation:

$$Uncertainty = \pm\sqrt{((pixel\ error)^2 + (georectification\ error)^2 + (digitizing\ error)^2)} \quad (4)$$

To account for these uncertainties in the final shoreline change output, weighted linear regression (WLR) was performed for each transect using Python. When performing WLR, the best-fit line was determined by assigning more emphasis to the more reliable data. To do so, the weight of each shoreline dataset was defined as a function of variance in the uncertainty of the measurement (Genz et al. 2007).

$$W = 1/e^2 \quad (5)$$

Where *e* is the shoreline uncertainty value. The rate of shoreline change is then defined as the slope of the best-fit line.

3.4. Coastal risk analysis

3.4.1. Exposure modelling

In the previous sections, asset change analysis and coastal inundation modelling was carried out for Nauru. The datasets obtained are summarised in Table 3.3. In this section, we determine the risk of Nauru's assets (buildings and roads) and population to being exposed to or damaged by coastal inundation. We investigated the risk of inundation for present climate conditions as well as under future sea-level conditions using projections from the IPCC AR6 projections of SSP1-1.9 and SSP5-8.5. In this assessment, projections for the years 2050 and 2100 were used.

Category	Datasets
Coastal inundation (grid resolution: 5 m)	Present • ARI 5 • ARI 10 • ARI 25 • ARI 50 • ARI 100 • ARI 250 • ARI 500 0.26 m SLR: SSP1-1.9 (2050) • ARI 5 • ARI 10 • ARI 25 • ARI 50 • ARI 100 • ARI 250 • ARI 500 0.61 m SLR: SSP1-1.9 (2100) • ARI 5 • ARI 10 • ARI 25 • ARI 50 • ARI 100 • ARI 250 • ARI 500 0.31 m SLR: SSP5-8.5 (2050) • ARI 5 • ARI 10 • ARI 25 • ARI 50 • ARI 100 • ARI 250 • ARI 500 1.07 m SLR: SSP1-1.9 (2100) • ARI 5 • ARI 10 • ARI 25 • ARI 50 • ARI 100 • ARI 250 • ARI 500
Asset change	Buildings • OSM 2020 polygon vector • PACRIS 2012 point vector Roads • OSM 2020 line vector
Population	2020 gridded population (Andrew et al. 2019), resolution 111 metres

Table 3.5: Nauru datasets used for risk assessment.

RiskScape, an open-source spatial data processing application for multi-hazard risk analysis (Paulik et al. in review), was used for risk assessment. In RiskScape, risk quantification is performed by building a model with assigned assets, hazards, and functions to analyse the exposure and vulnerability of the asset in a geospatial scale. Buildings, population data, and road length were used as assets for each of the coastal hazard scenarios.

Five RiskScape models were built to provide:

- Exposure of buildings using OSM 2020 data
- Exposure of road length using OSM 2020 data
- Exposure of population from SPC Statistics 2020 (Andrew et al. 2019)
- Exposure of buildings from the PACRIS 2012 database
- Economic loss from damaged buildings from the PACRIS 2012 database

These five models were used to simulate the various coastal inundation scenarios: present sea levels and future SLR projections (SSP1-1.9 and SSP5-8.5) at 5-, 10-, 25-, 50-, 100-, 250-, and 500-year return intervals.

Installation and setup of RiskScape software can be accessed through the online manual (https://riskscape.org.nz/docs/index.html). The models and functions used in this study are provided in Annex 1.

The first four models provide the level of exposure of assets (i.e., buildings, population, and roads) to the coastal inundation hazard. The last model was used to assess the economic risk and is detailed in the next section.

3.4.2. Risk modelling

To determine the risk of Nauru's buildings to coastal flooding, we assessed the potential damage and economic loss for each of the scenarios. Building types and replacement values (in 2012 USD) were obtained from the PACRIS 2012 database (https://risk.spc.int/). According to the U.S. Bureau of Labor Statistics (https://www.bls.gov/data/inflation_calculator.htm), the 2012 USD has inflated by 24% (i.e., USD 10 in January 2012 was worth USD 12.40 in January 2022).

Building damage was assessed using the fragility functions provided by Air Worldwide for the Pacific Catastrophe Risk Assessment & Financing Initiative (PCRAFI) project (PCRAFI 2013). The database (Annex 2) provides percentage of damage for different building types and different intensities of two hazards (storm surge and tsunamis). Wave-driven inundation is more destructive than classic storm surges (water rising over several hours); however, it is less destructive than tsunamis. In the present study, we performed damage and loss analysis for both storm surge water levels and tsunami water levels and used the average of the two. The lack of a robust regional damage function for wave-driven inundation is a well-known knowledge gap and should be addressed in future studies.

While the 2020 OSM dataset provides information about the location of buildings, it does not provide information on building types. To investigate the economic loss for 2020 assets we assessed exposure of and damage to buildings in 2012 and exposure of buildings in 2020. Assuming the distribution of building types across Nauru has been consistent since 2012 (last national-scale survey), we extrapolated the building damage from the 2012 assets to the 2020 assets. For instance, a 100-year flood event under current sea levels exposed 92 buildings in Meneng based on PACRIS 2012 and 111 buildings based on OSM 2020. This shows a building exposure growth of 21% over the 8 years. The exposure growth was then multiplied by the 2012 economic loss for the district to reflect the 2020 economic loss for building assets.

The annual expected damage for each district in Nauru was also determined. This was done by integrating the economic loss from the 5- to the 500-year ARI and then dividing it by 500 years.

4. Results

4.1. Coastal hazard

A maximum water level of 1.59 m (above the actual mean sea-level [MSL] datum) was recorded on 14 December 2001. This marks the highest measured water level by Nauru's tide gauge for the 1993–2021 period (Figure 4.1). The 30-day averaged time series reveals a strong mean sea-level variability mainly driven by ENSO, ranging from -30 to 37 cm. This is in line and in the same order of magnitude with previous estimates (e.g., Australian Bureau of Meteorology and CSIRO 2011). A relative long-term mean sea-level trend of 5.4 mm/year has been obtained, indicating a change well exceeding the global rate. This value is close to the value of 5.7 mm/year obtained by Allis et al. (2020) for the 1993–2019 period. Local direct measurements of vertical land movement have been completed by Geoscience Australia in support of the Sea Level and Geodetic Monitoring Project, providing an estimated subsidence rate in Nauru of 1.2 ± 1.5 mm/year. Storm surge data were obtained through wavelet analysis to isolate the part of the sea-level signal occurring in time scales larger than 12 and 24 hours. Storm surge usually refers to wind set-up and inverse barometric pressure in continental shelves; however, in remote isolated islands, wave set-up and infragravity waves due to swell dissipation generally dominate extreme TWLs and cause coastal inundation. These last two components (wave contribution) may be completely missed or at minimum, under-represented in tide gauge records. In the case of Nauru, a maximum storm surge of 0.503 m was recorded on 21 February 2014 due to the combination of wind and wave set-up associated with the development of a westerly wind burst on the western equatorial pacific, with offshore wave heights over 3 m (see Figure 4.1).

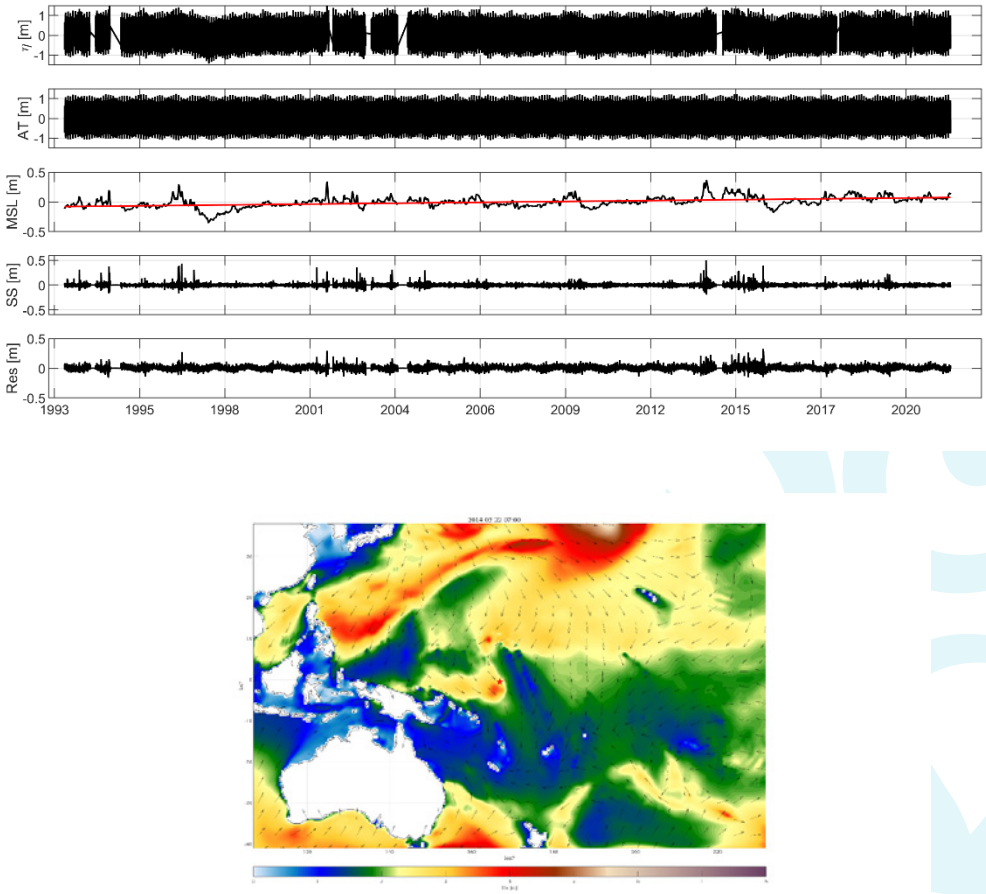

Figure 4.1: (top) Nauru tide gauge analysis. Raw hourly water level time series (η), astronomical tide (AT), mean sea level from 30 days smoothing window (MSL), storm surge from wavelet transform (SS) and residual (Res). (bottom) Map of significant wave height on 21 February 2014 from CAWCR wave hindcast.

Figure 4.2 shows the extreme value distribution of TWL at the present MSL for two points: the southeast (TWL up to 2.15 m above MSL) and the northeast of Nauru (TWL up to 2.5 m above MSL). As can be seen, although tradewind-generated waves from ENE to ESE dominate wave climate, they are bounded in height and period, preventing them from driving destructive extreme water level events. On the contrary, rare waves coming from the W and NW, generated by westerly wind bursts and deep extratropical storms in the North Pacific, are responsible for the highest extreme water level events that can affect Nauru.

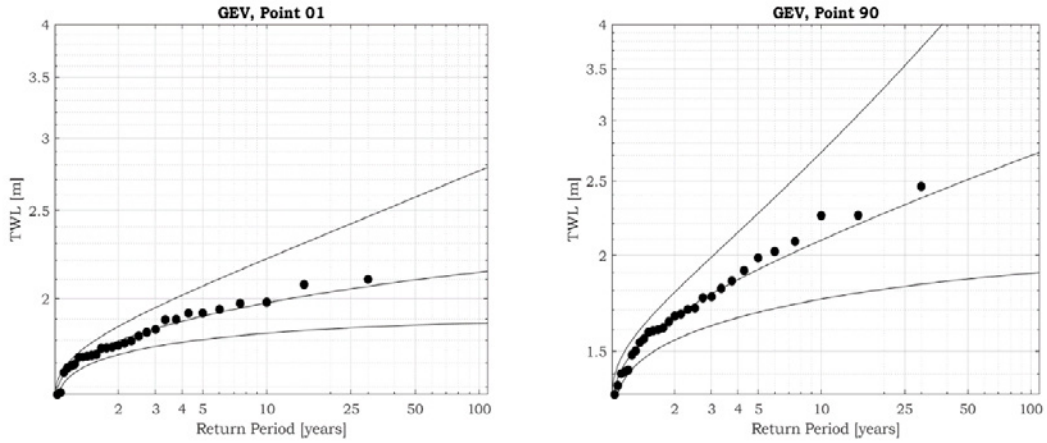

Figure 4.2: (Left) Extreme value distribution of TWL at the southeast and (right) the northwest of Nauru.

A quadratic surface was fitted to account for associated TWL variability related to different wave exposures and return intervals. These surfaces were intersected ("bathtub" approach) with the 5-m resolution DEM of Nauru, obtaining inundation maps as the one shown in Figure 4.3 for the 100-year ARI event at the present mean sea level.

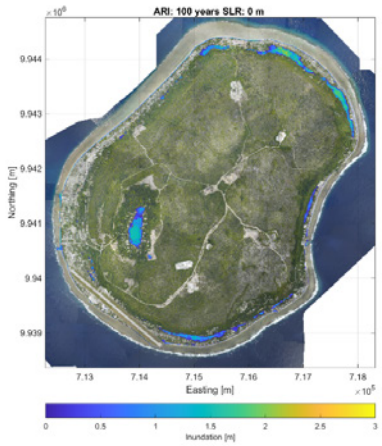

Figure 4.3: 100-year ARI coastal inundation map of Nauru.

The bathtub model assumes adjacent direct connectivity between grid cells to simulate overland flows, neglecting terrain roughness, timing/duration of the event and flow velocity. This technique can lead to overpredictions due to simplification of physical processes, potentially exaggerating socioeconomic damage. However, for the sake of simplicity and due to lack of bathymetry data to downscale the wave fields surrounding Nauru, it was deemed valid for this study. The inner island lagoons across Nauru are known to be tidally responsive (Allis et al. 2020), which means that changes in offshore water levels are transmitted (albeit in a dampened manner) to the lagoons via underwater connections between the lagoons and the ocean. Although tidal efficiency (the damping of tide levels due to distance to the sea and geological properties) is larger for low frequency sea-level variations such as sea-level anomaly and sea-level rise, this is not entirely true for tides or wave setup/runup that vary in shorter time scales. Therefore, lagoon inundation may be exaggerated or overpredicted in this study.

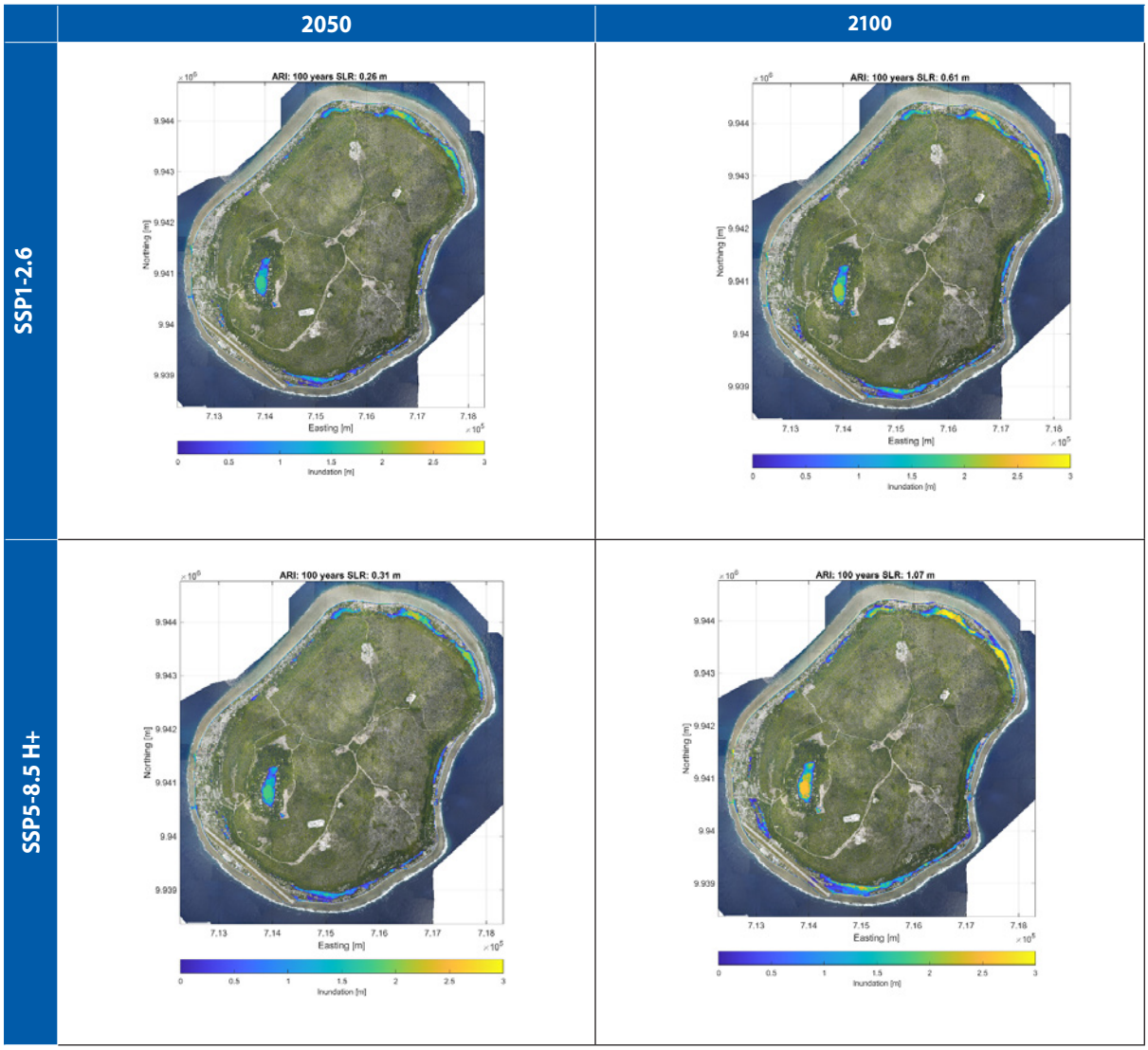

Figure 4.4: 100-year ARI coastal inundation maps of Nauru for 2050 and 2100 and for SSP1-2.6 and SSP5-8.5 H+ scenarios.

Figure 4.4 shows the 100-year ARI inundation for 2050 and 2100 and for the SSP1-2.6 and SSP5-8.5 H+ scenarios. The northern and southern tip of Nauru are more prone to coastal inundation as they are lower lying. Furthermore, they show a larger hydraulic connectivity with the ocean. Nauru, like other uplifted limestone islands, is quite safe from coastal inundation, with only a narrow fringe along the coastline being affected by the action of waves and sea-level anomalies. It is only under the most unfavourable considered scenario (SSP5-8.5 H+ in 2100) with 1.07 m SLR when larger patches of land connected to the ocean start being inundated. For the most favourable scenarios, most of the inundation is the result of elevated water levels in lagoons, which can also result in increased assets and population exposure to future flooding hazards.

4.2. Change in assets

4.2.1. Buildings

There has been a significant increase in coastal buildings and developments over the eight years between 2012 and 2020. Overall, the number of buildings has increased in all districts from 2746 to 4314 (50.91%). Four districts recorded > 100% growth: Anabar, Anibare, Ewa and Ijwa. Five districts recorded between 50–100% growth, and five districts recorded < 50% growth (Figure 4.5).

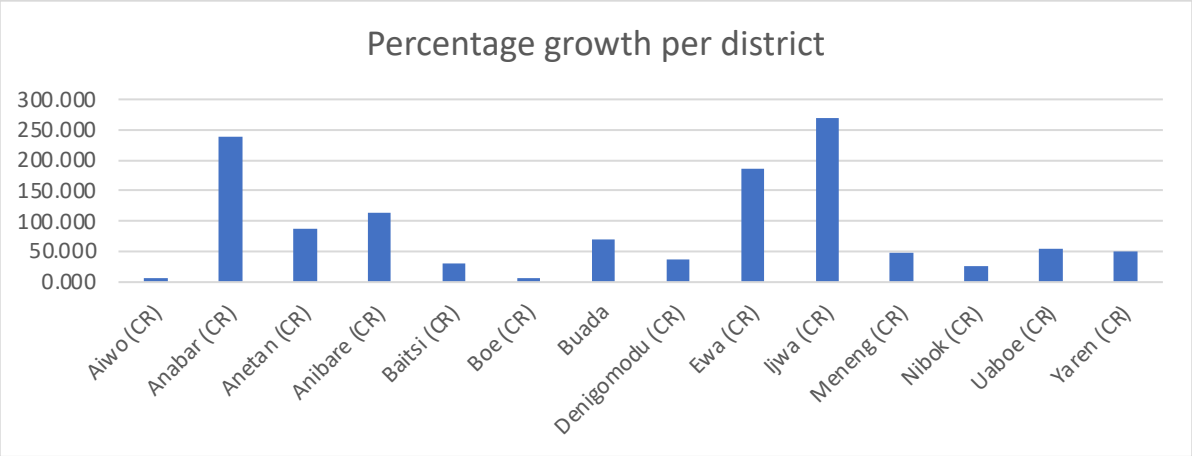

Figure 4.5: Percentage growth of buildings per district between 2012–2020. CR = coastal region.

However, in the four districts recording the highest increase in buildings, most new structures were developed in the central regions of Nauru.

The 2020 building data was overlaid with the 2020 population grid (Andrew et al. 2019) and as expected, there was a clear correlation between population density and building structures (Figure 4.6).

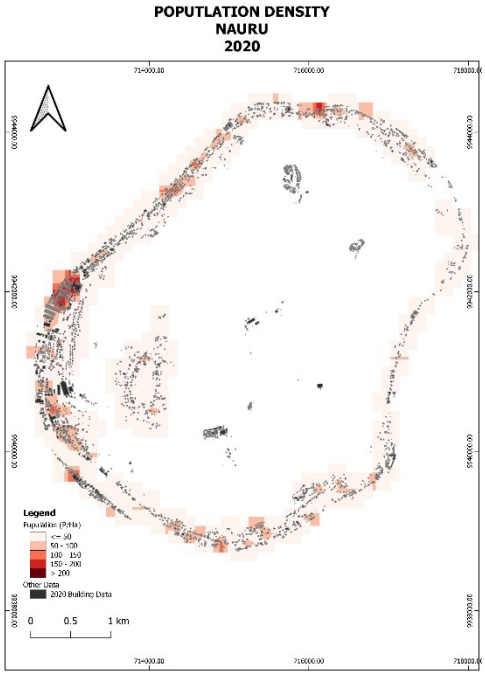

Figure 4.6: 2020 population density against 2020 building data.

4.2.2. Seawall change analysis

The overall length of seawalls increased over the same time span, with most new seawall sections built in Uaboe, Ewa and Ijuwa (Figure 4.7). However, most of Nauru's coastline is still without seawalls. For example, in the district of Uaboe, there are only two small sections of coastline protected by seawalls (Figure 4.8), with the bigger of the two sections built after 2014, resulting in the large increase in seawall length displayed in Figure 4.7.

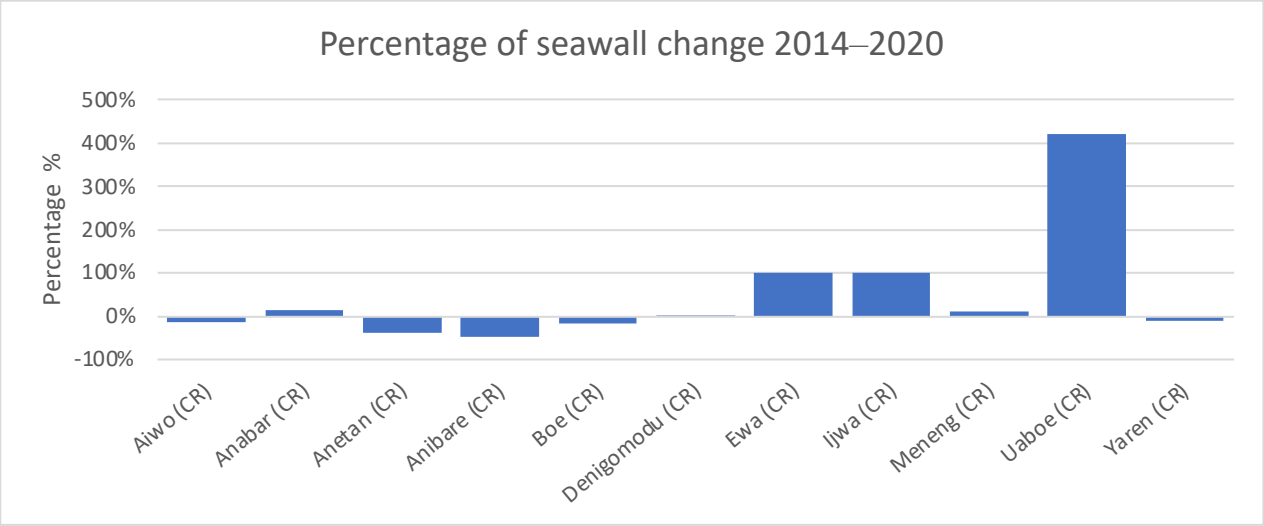

Figure 4.7: Percentage of seawall change per district between 2014–2020. CR = coastal region.

Figure 4.8: Newly built seawall at Uaboe district.

4.2.3. Population trends

For most of the districts, there was an increase in population between 1992 and 2019. Overall, the population increased by 19.87%, with Baitsi showing the largest population growth (by percentage) followed by Anibare and Anetan (Figure 4.9). Exceptions were the districts of Denigomodu and Nibok, where the population decreased between 1992 and 2019. However, when investigating the different time slices for which population data were available, more variability in the districts was observed. From 1992 to 2002 the population decreased in several districts, notably in Ijuw, Nibok and Uaboe, while there was a significant increase in Baitsi, with population growth

of more than 150% (Figure 4.10). Moreover, between 2002 and 2011, there was a minimal increase in population for most of the districts. The districts of Anabar, Anetan, Batsi, Aiwo, Boe and Yaren showed the largest growth, while Uaboe, Denigodmodu and Anibare recorded a decrease during the same period. Between 2011 and 2019, Anabar was the only district that showed a decrease in population. Positive population growth was noted in most of the districts, with Uaboe and Anibare showing the greatest growth with an increase of > 40%.

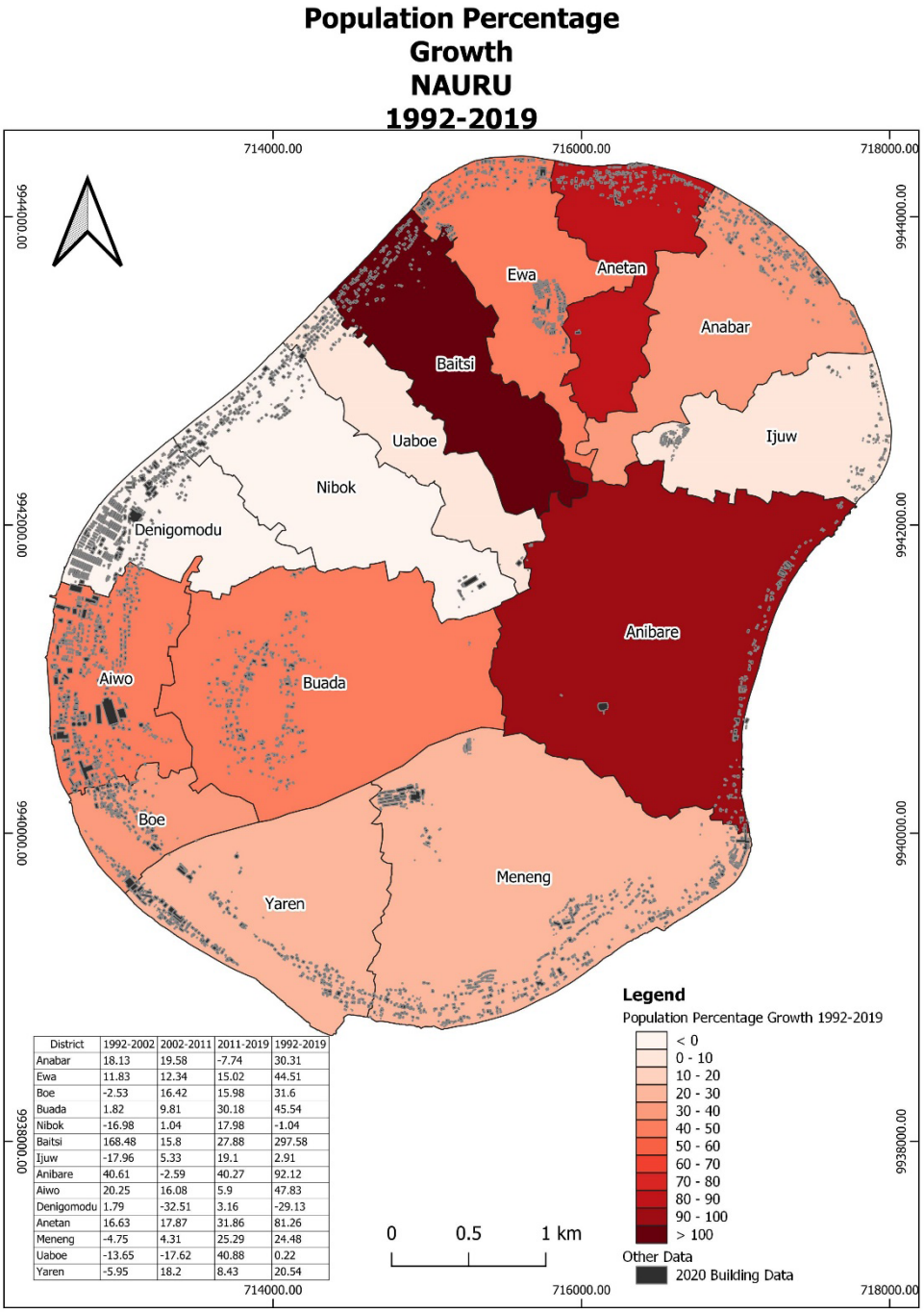

District	1992-2002	2002-2011	2011-2019	1992-2019
Anabar	18.13	19.58	-7.74	30.31
Ewa	11.83	12.34	15.02	44.51
Boe	-2.53	16.42	15.98	31.6
Buada	1.82	9.81	30.18	45.54
Nibok	-16.98	1.04	17.98	-1.04
Baitsi	168.48	15.8	27.88	297.58
Ijuw	-17.96	5.33	19.1	2.91
Anibare	40.61	-2.59	40.27	92.12
Aiwo	20.25	16.08	5.9	47.83
Denigomodu	1.79	-32.51	3.16	-29.13
Anetan	16.63	17.87	31.86	81.26
Meneng	-4.75	4.31	25.29	24.48
Uaboe	-13.65	-17.62	40.88	0.22
Yaren	-5.95	18.2	8.43	20.54

Figure 4.9: Population percentage growth between 1992–2019 per district.

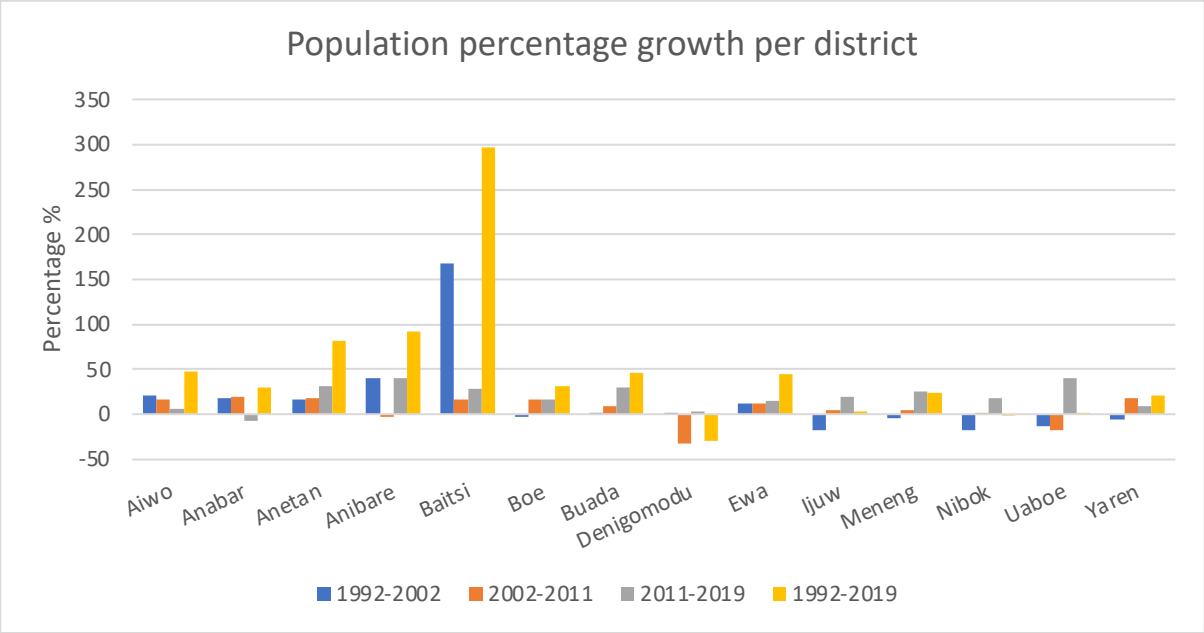

Figure 4.10: Short-term and long-term population growth per district.

4.3. Shoreline change

Through the R software package AMBUR, a total of 377 transects were constructed to capture shoreline movement using watermark as the shoreline proxy. Historical shorelines over a 28-year period were extracted from satellite images for the years 1992, 2005, 2010, 2014, 2018 and 2020.

Using the watermark as the shoreline proxy, about 41% of the shoreline around Nauru showed erosion, while 59% showed accretion. As shown in Figure 4.11, the WLR rates ranged from −0.73 m/year to 2.65 m/year, and the average rate of change was recorded as 0.01 m/year for the overall outlook of Nauru. Nauru's shoreline shows variable erosion and accretion around the island, as seen in Figure 4.11. However, the average rates of change for each district show that eroding shorelines are mainly near the north-eastern and southern parts, while accretion is found mostly on the western and eastern side of the island of Nauru (Figure 4.12).

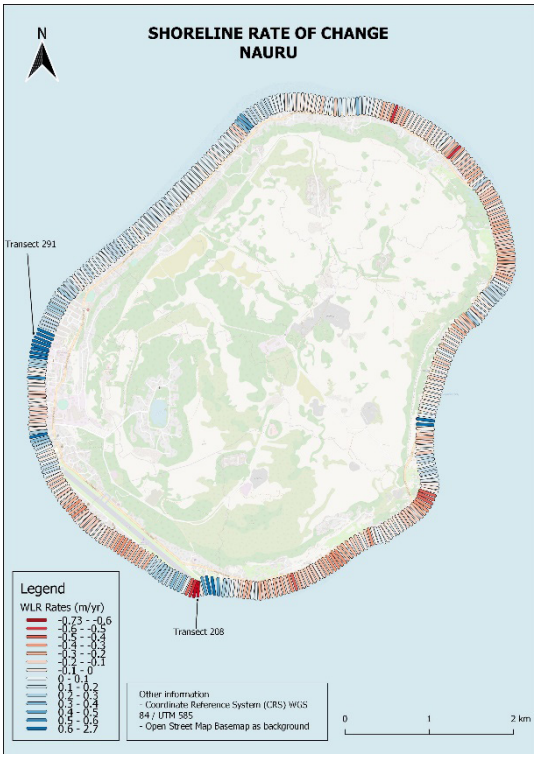

Figure 4.11: Transects showing weighted linear regression rates for Nauru. Blue indicates areas of accretion, while red indicates areas of erosion. Transects 291 and 208, which are labelled, show the largest accretion and erosion, respectively.

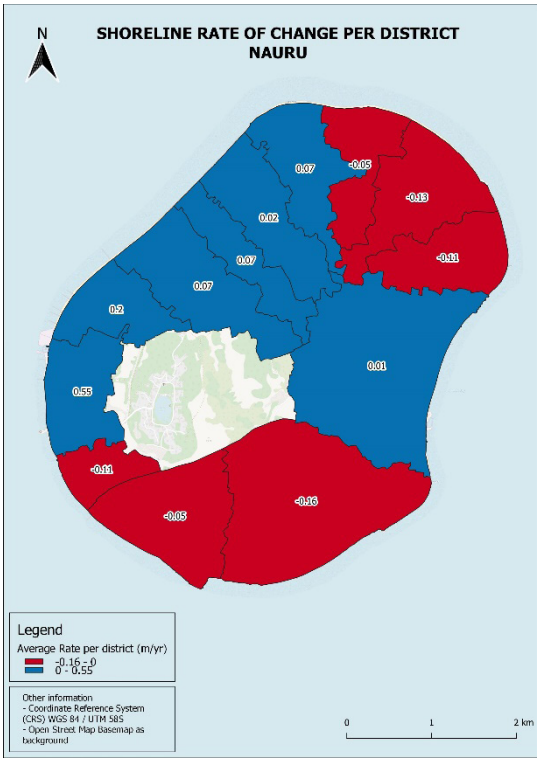

Figure 4.12: Average rate of change for each coastal district in Nauru.

Major shoreline erosion was noted around the southern tip of the island at the edge of the airport, with an erosion rate of −0.73 m/year. A closer look at the data indicates that there was a high erosion event between 1992 and 2005, after which the shoreline stabilised (Figure 4.13). Since the construction of the airport extension was completed in the early 1990s (Maharaj 2000), it is likely that shoreline changes between 1992 and 2005 are a result of the construction. At the same time, major accretion was found along the western coastline, with an accretion of 2.66 m/year. However, time series analysis (Figure 4.14) indicates a relatively stable coastline between 1992 and 2018 and a sharp increase in accretion between 2018 and 2020. The accretion of shoreline is linked to the reclamation of land for the construction of a new port (Figure 4.15).

These two examples illustrate that the largest shoreline changes in Nauru are mainly driven by episodic events over short time frames that override any potential long-term trends (e.g., from climate change). In order to obtain more conclusive insight on how climate change and climate variability may impact shoreline change in Nauru, a longer shoreline dataset at higher sampling frequency would be required. Furthermore, a more in-depth study should investigate the effects of seawalls on nearby shorelines as it is commonly known that shoreline stabilisation through construction of seawalls often lead to coastal erosion along adjacent beaches.

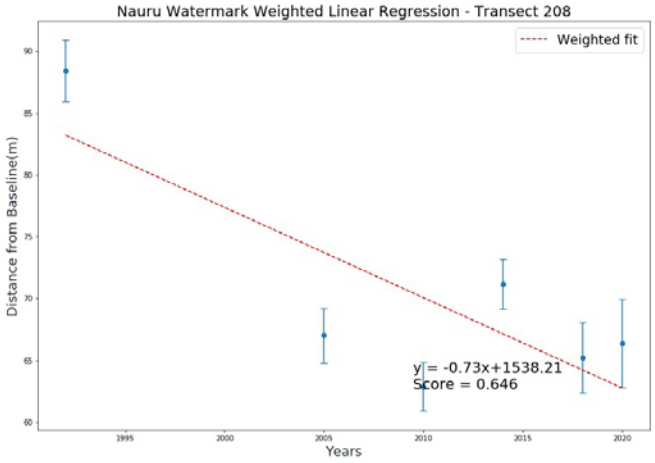

Figure 4.13: Weighted linear regression rate for the transects showing the greatest erosion.

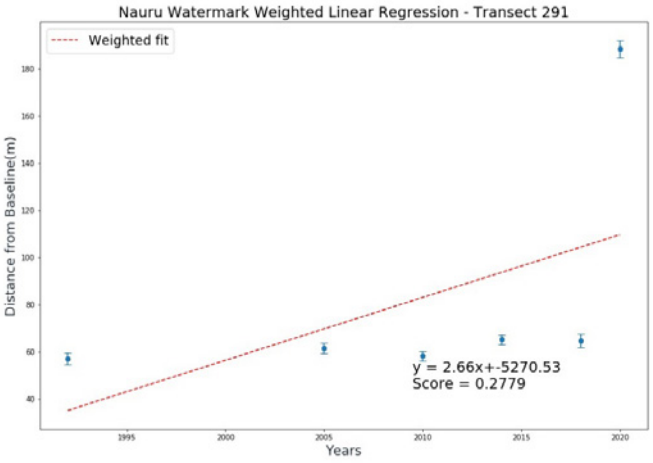

Figure 4.14: Weighted linear regression rate for the transects showing the greatest accretion.

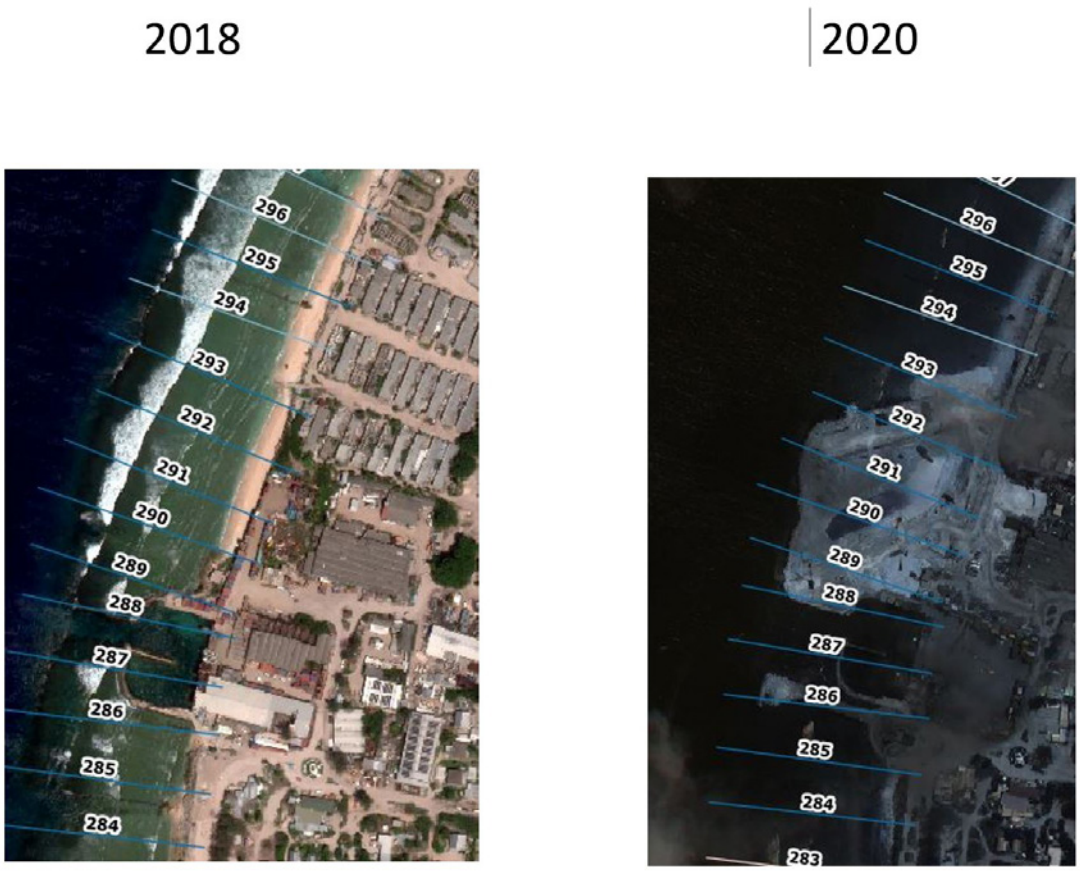

Figure 4.15: Aerial images of the western coastline of Nauru for 2018 and 2020.

4.4. Coastal risk

4.4.1. Exposure of assets to the coastal inundation hazard

Through RiskScape, data for Nauru's buildings, roads and population were exposed to modelled coastal inundation from the present climate sea levels and SLR projections. We considered 5-, 10-, 25-, 50-, 100-, 250- and 500-year return intervals. The number and percentage of exposed buildings and population, as well as the length of exposed roads, was assessed for each of the scenarios.

Table 4.1 provides the total number of buildings and population in 2020 (based on OSM 2020) and the total number of buildings from PACRIS 2012. In addition, Annexes 3–7 provide the number of exposed buildings, population and road length per district using OSM 2020 data. Annex 8 provides the number of exposed buildings per district based on 2012 PACRIS data.

No.	District	Total buildings per district (2012)	Total buildings per district (2020)	Total population per district (2020)
1	Aiwo	532	566	1570
2	Anabar	93	316	435
3	Anetan	137	257	207
4	Anibare	96	208	261
5	Baitsi	119	158	644
6	Boe	201	217	1220
7	Buada	171	289	1103
8	Denigomodu	283	386	1885
9	Ewa	138	393	529
10	Ijuw	54	200	201
11	Meneng	449	660	1441
12	Nibok	181	225	554
13	Uaboe	74	110	391
14	Yaren	218	329	703
	TOTAL	**2746**	**4314**	**11144**

Table 4.1: Total number of buildings and population per district from OSM 2020 and total number of buildings from PACRIS 2012.

Nauru is relatively exposed to coastal inundation, with most development and 93% of Nauru's population residing within 1 km of the coast (Andrew et al. 2019). A 5-year ARI inundation event directly impacts 46% of Nauru's population, flooding 6.2% of buildings and 2.7 km of roads (Annexes 3–5). A 100-year ARI inundation event impacts 54% of Nauru's population, flooding 9.2% of buildings and 3572 m of roads. The most extreme scenario (500-year ARI event) impacts 58% of Nauru's population, flooding 10.8% of buildings and 4297 m of roads. Sea-level rise clearly exacerbates the risk of coastal flooding, with 59% of people, 16.7% of buildings and 8.1 km of roads expected to be directly impacted by a 5-year ARI event by 2100 (under the SSP5-8.5 scenario). A 500-year ARI event (an event with a 0.2% annual probability) under the SSP5-8.5 scenario (2100 horizon) results in 66% of Nauru's population impacted, with flooding affecting 29.3% of buildings and 15.3 km of roads. A detailed analysis by district is provided below.

Present sea level

During a 100-year ARI event at the present sea level, the district with the highest population exposure is Meneng (1317 people), followed by Boe (861 people). Even though these two districts have the highest number of exposed individuals, this accounts for 91% of Meneng's population and 71% of Boe's, while the smaller district of Anetan shows 100% population exposure as all 207 people in that district are exposed. Other districts show similar high percentages of population exposure, including Nibok (83%), Anibare (83%), Ijuw (86%) and Ewa (93%).

The district with the highest number of exposed buildings during a 100-year ARI event is also Meneng, with 111 (17%) buildings exposed. This is followed by Anabar (99/31% buildings), Anetan (43/17% buildings), Ewa (48/12% buildings), Anibare (23/11% buildings) and Boe (21/10% buildings).

Coastal inundation also significantly impacts transport infrastructure such as roads across all districts. During a 100-year ARI event, flooding affects 914 m of road in the district of Anabar, followed by Anibare (905 m), Meneng (594 m), and Anetan (506 m). Further breakdown of different inundation scenarios can be found in Figure 4.16.

Future projections

The impact of coastal flooding on population, buildings and roads for various return intervals was investigated for different climate change projections under the SSP1-1.9 and SSP5-8.5 scenarios with 2050 and 2100 horizons.

The population exposure for all SLR projections in 2050 and 2100 reveal a similar pattern to present sea levels in regard to the most exposed districts (Figures 4.17–4.20). For the worst-case climate change scenario (SSP5-8.5 2100 horizon) at a 100-year ARI event, the highest impact is seen in Meneng, with 1338 (93%) people affected. This is followed by Boe (950 people, 78%), Aiwo (798 people, 51%) and Baitsi (572 people, 89%). The highest percentage of population exposure is found in the districts of Anabar, Anetan and Uaboe (100% each).

With increased sea levels at the most extreme SLR scenario (SSP58-8.5 by 2100 at a 100-year ARI event), Meneng district has the most exposed buildings (257 buildings/39%). This is followed by Anabar, with 181 exposed buildings (57%, the highest percentage of buildings exposed per district), Yaren (117 buildings, 36%), Anetan (87 buildings, 34%) and Ewa (90 buildings, 23%).

Under the SSP5-8.5 SLR scenario (2100 horizon) at a 100-year ARI event, the most impacted district in terms of inundated roads is Meneng, with 2620 metres of road exposed. This is followed by Anabar with 2135 m, Anibare (1925 m) and Anetan (1225 m). A detailed breakdown of exposure can be found in Figures 4.17–4.20 and in Appendix 7.

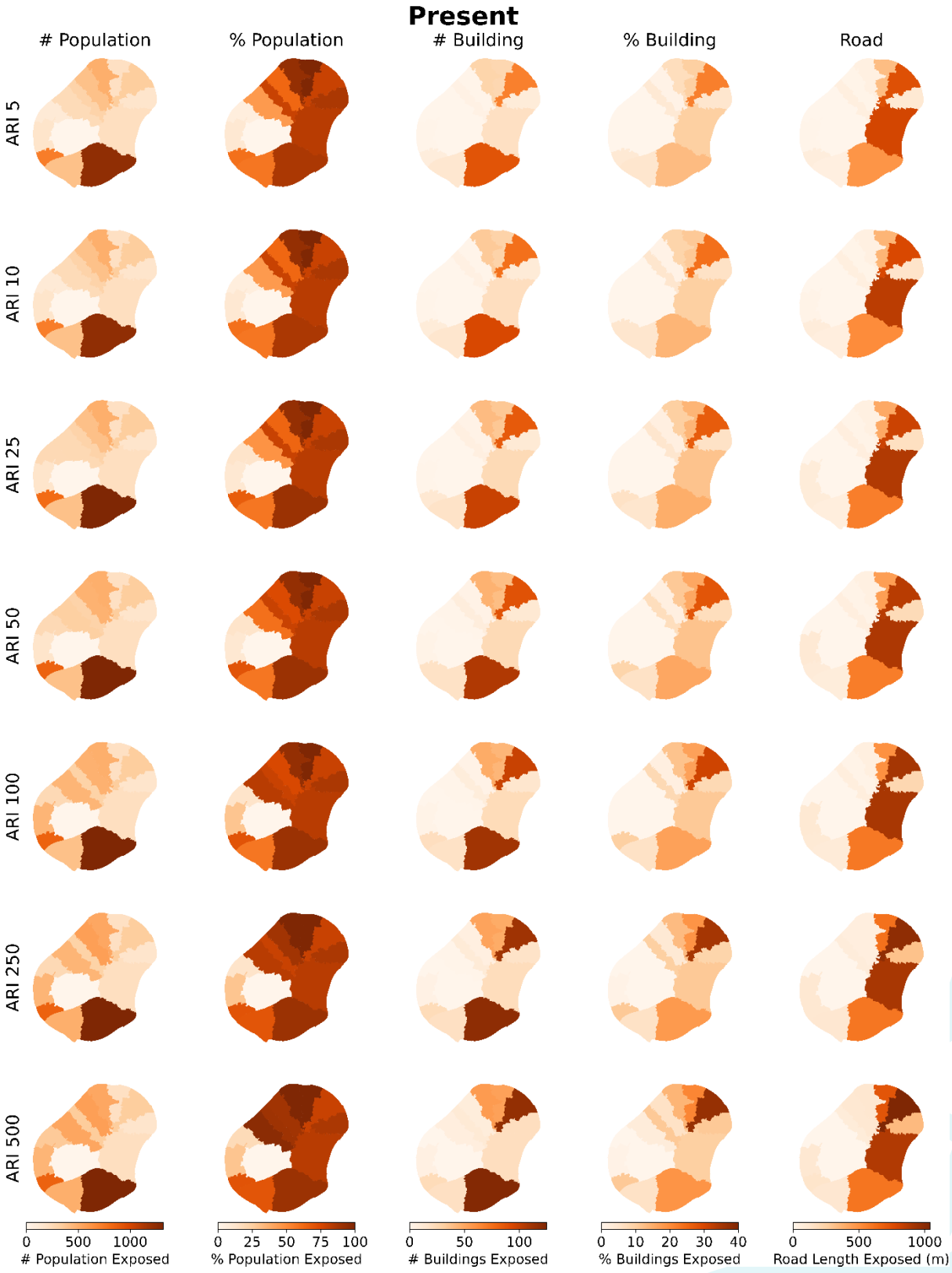

Figure 4.16: Exposure of population, buildings and roads for present projection at ARI 5, 10, 25, 50, 100, 250 and 500 years (OSM 2020 building dataset).

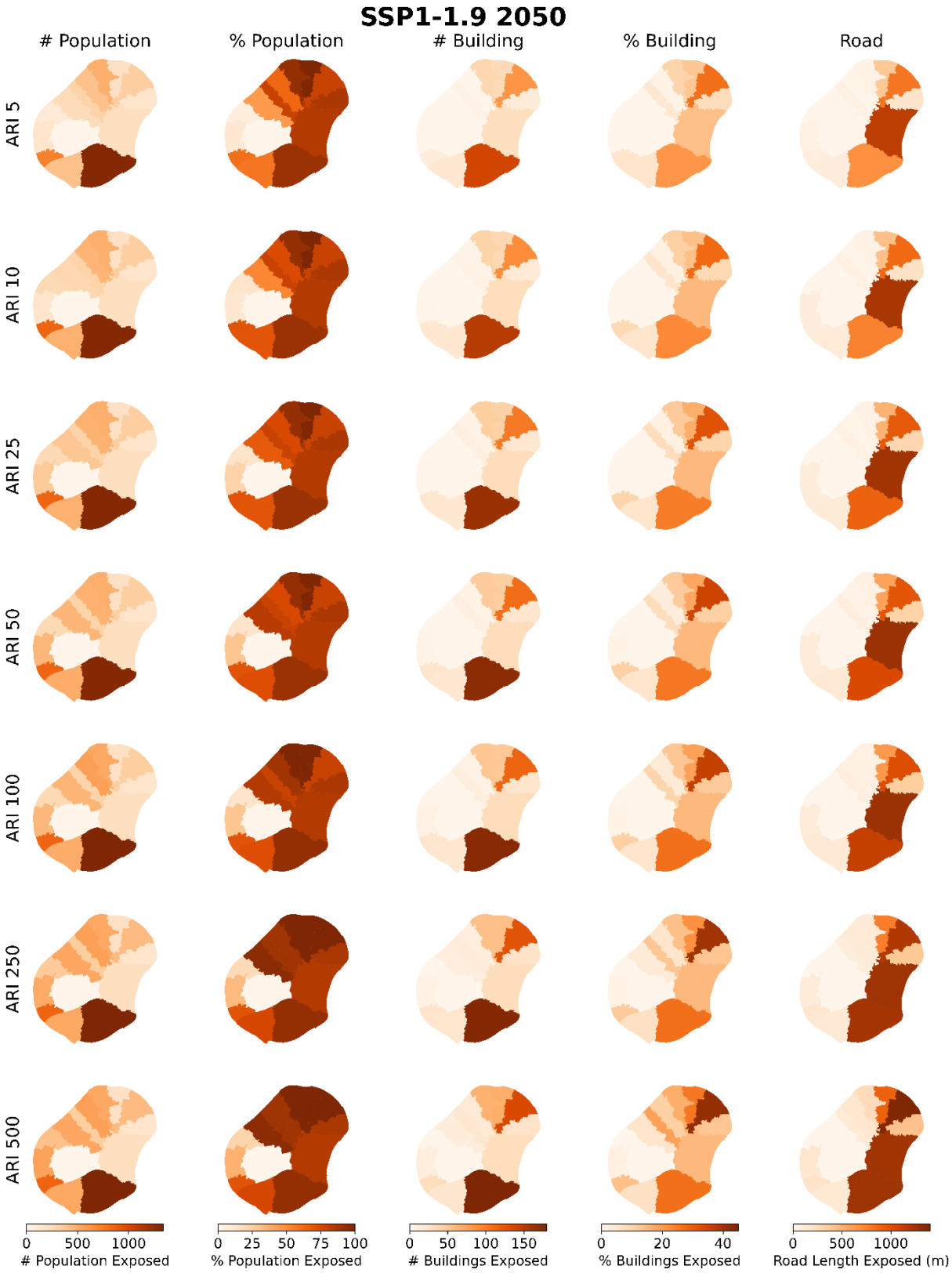

Figure 4.17: Exposure of population, buildings and roads for SLR projection (SSP1-1.9 2050) at ARI 5, 10, 25, 50, 100, 250 and 500 years (OSM 2020 building dataset).

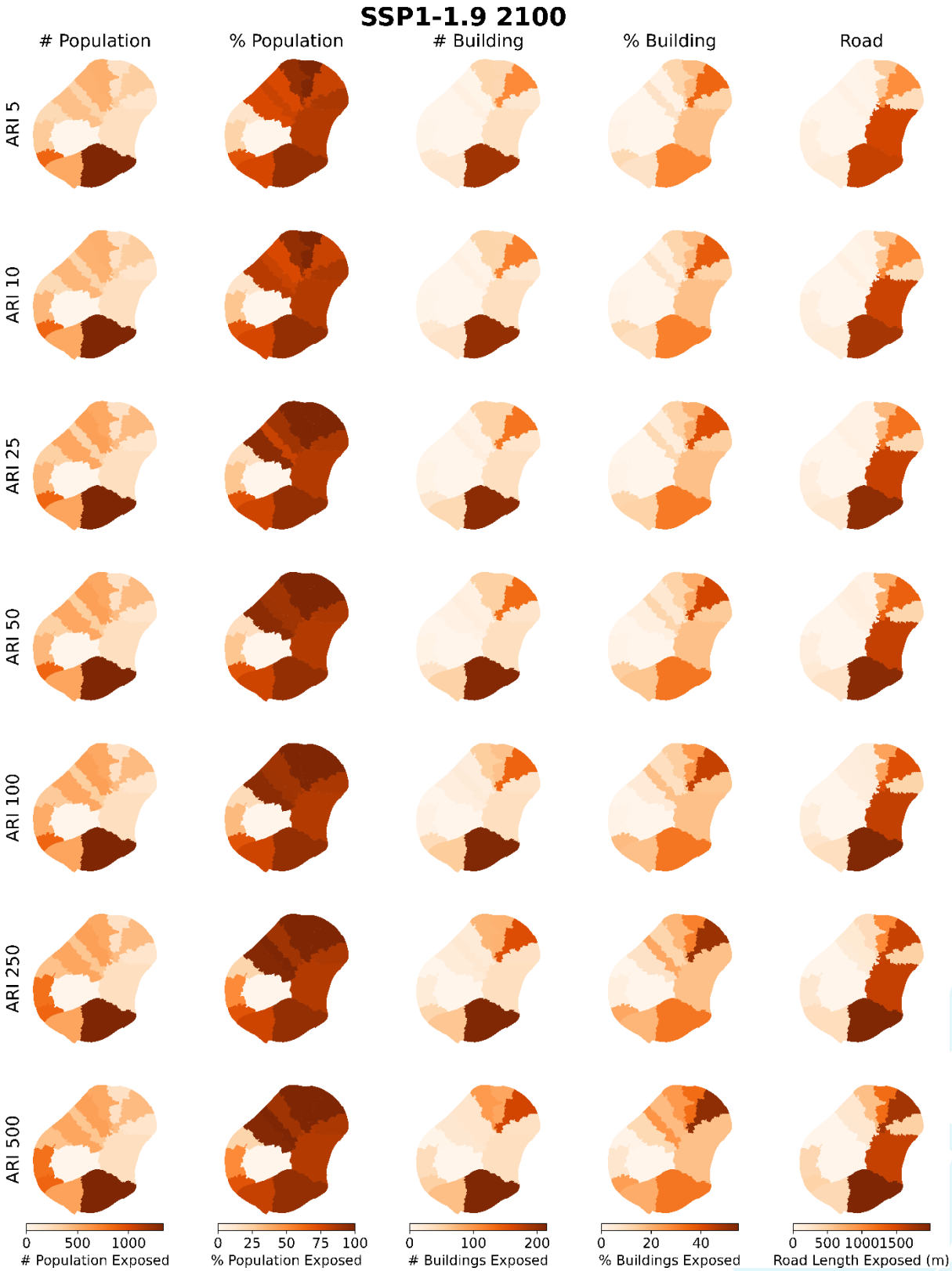

Figure 4.18: Exposure of population, buildings and roads for SLR projection (SSP1-1.9 2100) at ARI 5, 10, 25, 50, 100, 250 and 500 years (OSM 2020 building dataset).

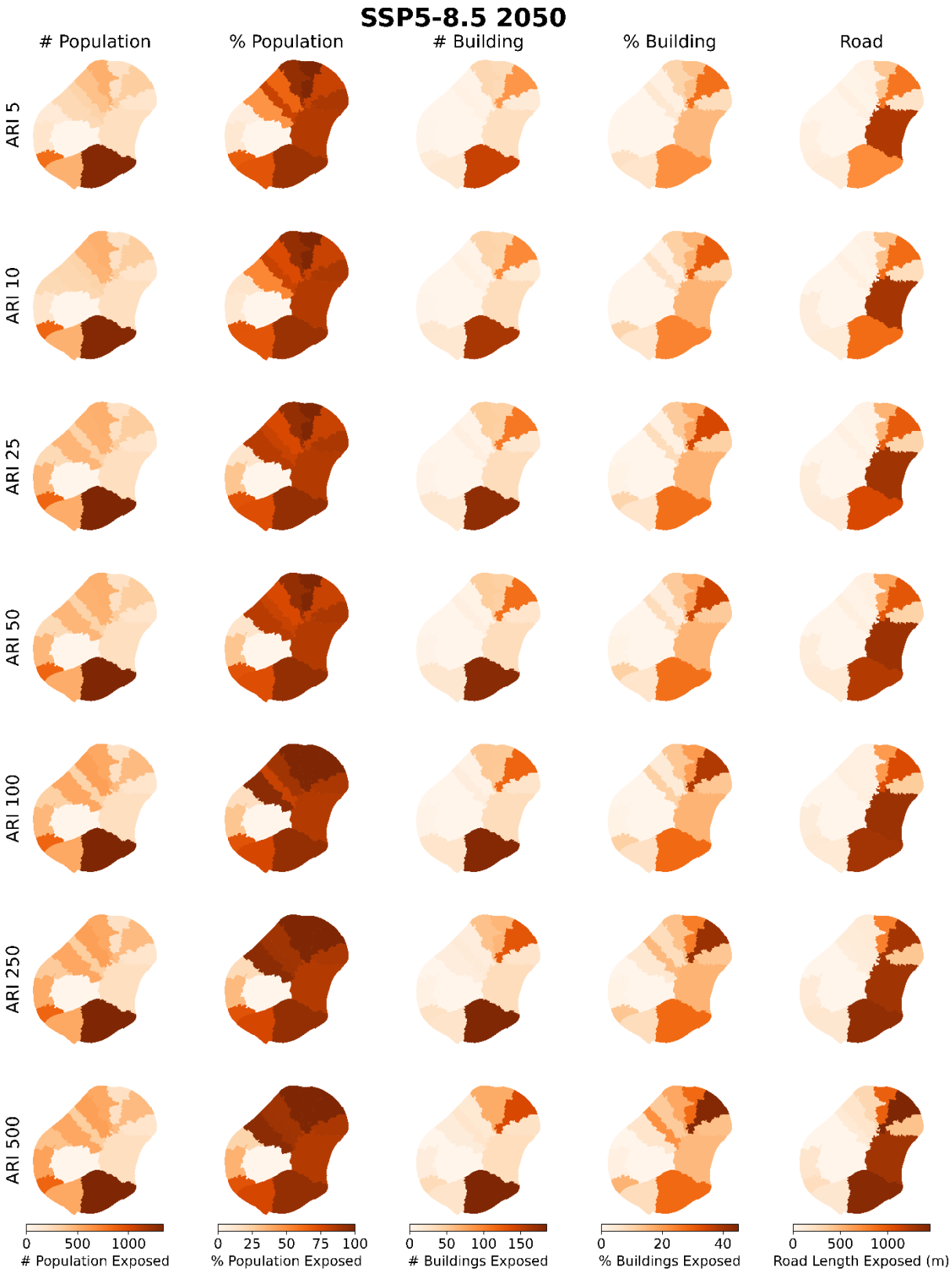

Figure 4.19: Exposure of population, buildings and roads for SLR projection (SSP5-8.5 2050) at ARI 5, 10, 25, 50, 100, 250 and 500 years (OSM 2020 building dataset).

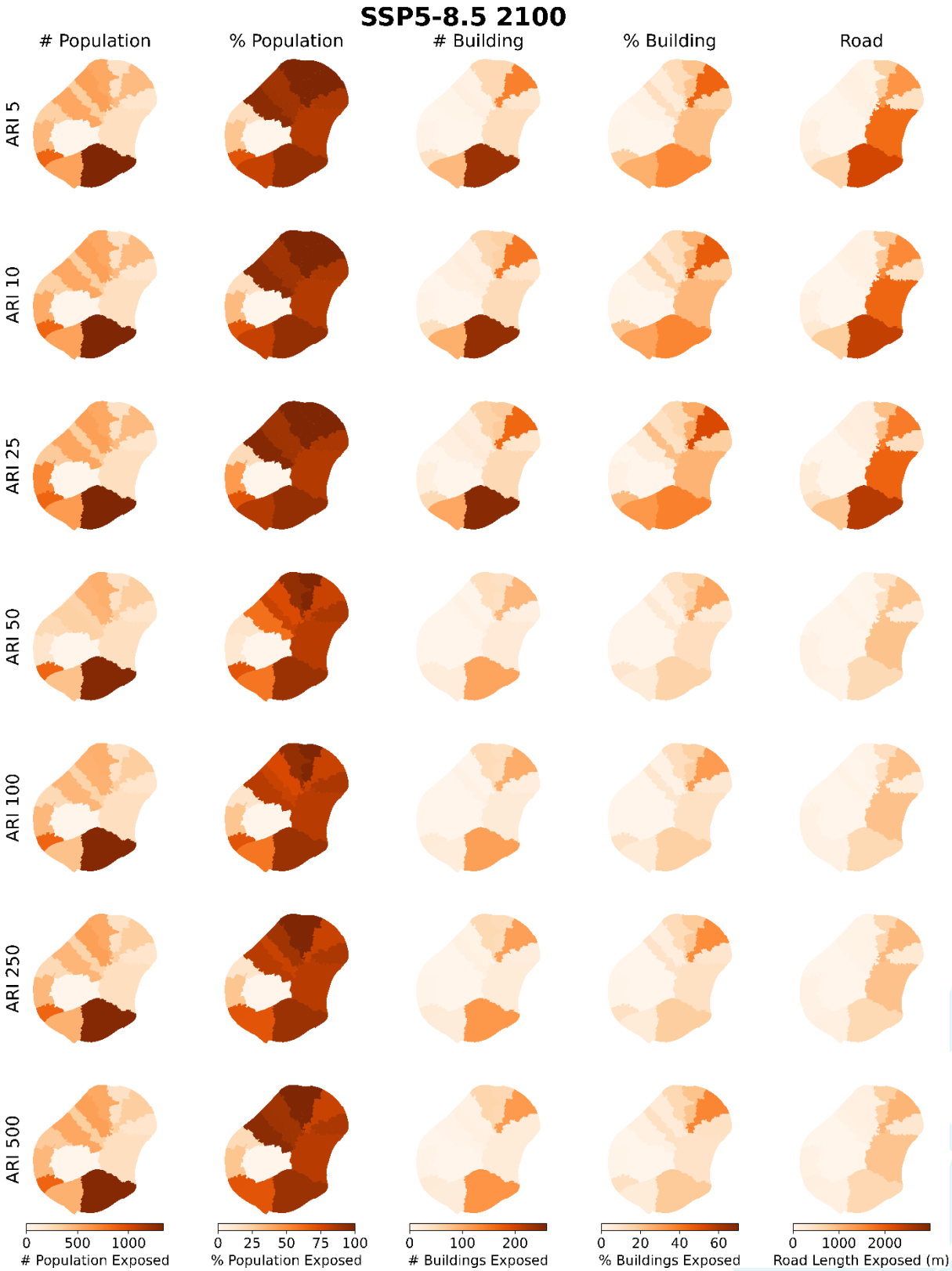

Figure 4.20: Exposure of population, buildings and roads for SLR projection (SSP5-8.5 2100) at ARI 5, 10, 25, 50, 100, 250 and 500 years (OSM 2020 building dataset).

4.4.2. Economic loss from coastal inundation

Economic losses are based on the estimated damage to buildings and the expected replacement costs. Figure 4.21 provides the location and damage state of buildings for each scenario. Most of the damage occurs along the north- and south-eastern coasts of Nauru. In particular, the buildings in Ewa, Anetan and Anabar in northern Nauru, and Meneng and Yaren in south-eastern Nauru are expected to experience the most serious damage. In comparison, the western coast of Nauru is sheltered, and there is less extreme damage to buildings.

Figure 4.22 provides the estimated economic loss for different ARIs for present sea levels and for 2050 and 2100 projections (with the different socioeconomic pathways). The upper range of the error bars reveals economic loss incurred from the tsunami fragility function and the lower range shows loss from the storm surge fragility function. In the following analysis, we assume that the damage lies in the middle of the two. For present sea levels, the estimated loss varies between USD 2.7 million (for the 5-year ARI) and USD 9.5 million (for the 500-year ARI). By 2050, the estimated loss increases slightly to between USD 4.7 million (for the 5-year ARI under the SSP1-1.9 scenario) and USD 14.3 million (for the 500-year ARI under the SSP5-8.5 scenario). This range increases even further by 2100 when estimated monetary losses are expected to range between USD 9.7 million (for the 5-year ARI under the SSP1-1.9 scenario) and USD 30.4 million (for the 500-year ARI under the SSP5-8.5 scenario). A detailed breakdown is available in Annex 9.

The expected annual damage was then determined for all of Nauru, as well as for each district. Under present sea-level conditions, the annual expected loss from coastal flooding for the whole of Nauru is approximately USD 1.3 million/year. This value is expected to increase with sea-level rise. By 2050, we estimate an annual loss ranging between USD 2.2 million/year (SSP1-1.9) and USD 2.4 million/year (SSP5-8.5). By 2100 the expected annual loss increases even further, ranging between USD 4.2 million/year (SSP1-1.9) and USD 7.3 million/year (SSP5-8.5).

Figure 4.23 provides the annual loss per district, with error bars reflecting the upper limit range incurring from the tsunami fragility function and the lower limits from the storm surge fragility function. The mean of both fragility functions is represented as bar plots. Buada and Denigomodu are not represented in this plot as there is little to no damage to these districts.

At present sea levels, the highest annual expected damage is in Anabar district (USD 0.4 million/year), followed by Meneng (USD 0.3 million/year). By 2050, the annual expected damage in Anabar increases to between USD 0.6 million/year (SSP1-1.9) and USD 0.7 million/year (SSP5-8.5), followed by Meneng with between USD 0.5 million/year (SSP1-1.9) and USD 0.6 million/year (SSP5-8.5). The expected annual damage increases significantly under 2100 projections, with highest expected annual damage observed in Meneng (between USD 1.28 million/year and USD 2.4 million/year for the SSP1-1.9 and SSP5-8.5 scenarios, respectively), followed closely by Anabar with an annual expected loss of USD 1.25 million/year (SSP1-1.9) to USD 1.9 million/year (SSP5-8.5).

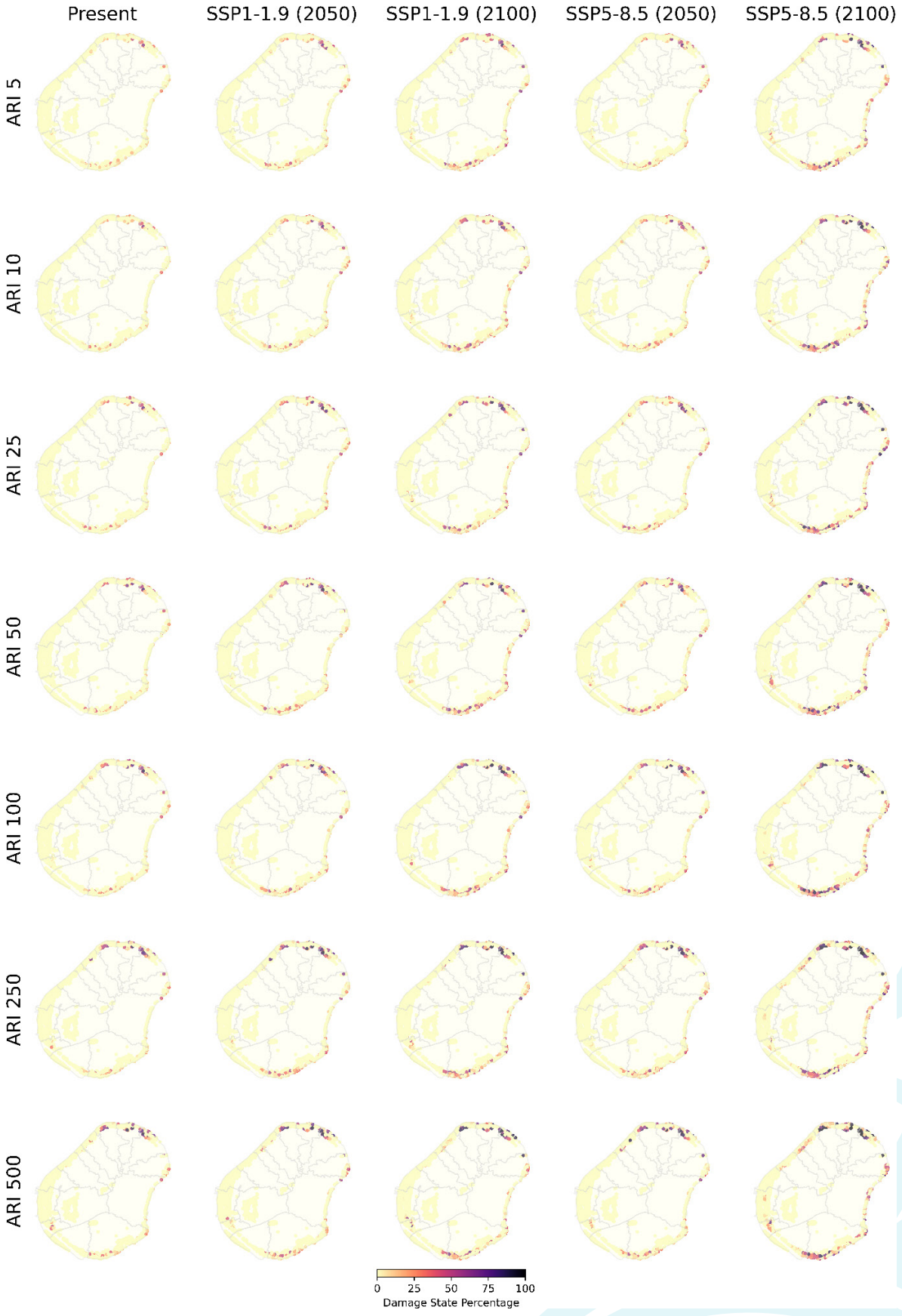

Figure 4.21: Percentage of damaged buildings (2012 PACRIS building data) for the present and SLR projections of coastal inundation hazard at ARI 5, 10, 25, 50, 100, 250 and 500 years.

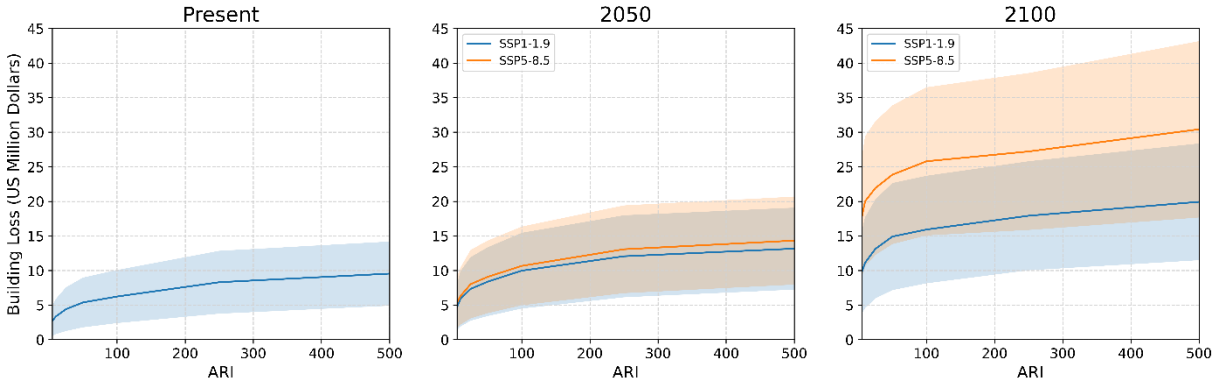

Figure 4.22: Building economic loss curve for the present (left), 2050 (middle) and 2100 (right). The SLR projections for SSP1-1.9 and SSP5-8.5 are compared in the 2050 and 2100 plot. Upper limits reveal the economic loss associated from the tsunami fragility function and the lower limits for the storm surge fragility function.

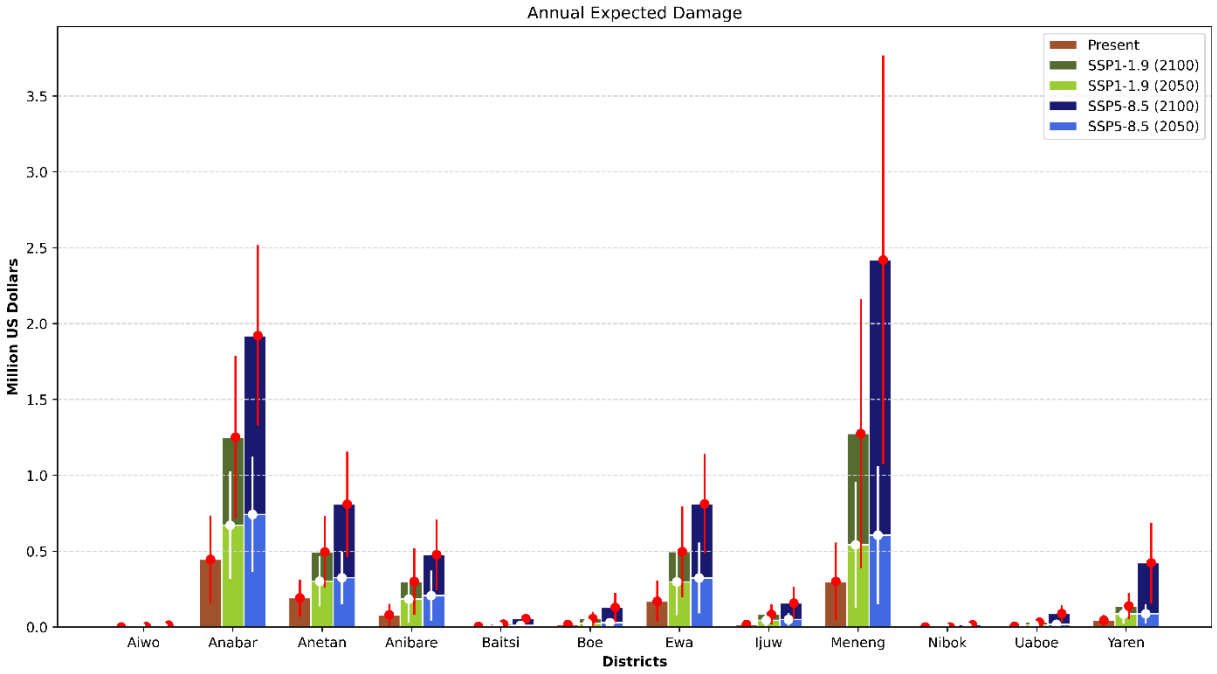

Figure 4.23: Annual expected damage loss incurred for each Nauru district. The plot shows the annual loss each district may incur for 2020 using the 2012 US dollar valuation. Upper limits reveal the inferred loss from a tsunami fragility function with lower limits for the storm surge fragility function. The Buada and Denigomodu districts are not plotted as little to no buildings are exposed to the hazard.

5. Discussion

In the present study, we investigated the risk to Nauru's population and infrastructure from coastal flooding and shoreline change, differentiating between anthropogenic and climate change-related causes of risk.

For the first time, wave-driven flooding was considered as a quantified hazard in Nauru. The results indicate a significant risk to infrastructure and population from coastal inundation. Elevated sea levels are expected to result in an exacerbation of risk as larger areas will be affected by coastal flooding, leading to an increase in exposure of population and assets. This will lead to a rise in anticipated annual damage and loss to buildings across Nauru, with the districts Anabar and Meneng expected to suffer the largest financial loss.

The results show a significantly higher exposure of population compared to buildings. This disproportion can be attributed to the differences in spatial resolution of the underlying datasets. While each building was digitized individually, population data were provided on a 111-metre by 111-metre grid. The coarseness of population data may lead to a significant overestimation of exposed population during inundation events. Building exposure may therefore be a better proxy for population exposure as it can be assumed that people live equally distributed across the buildings. This issue should be explored further in future studies to attempt to account for this discrepancy.

While there is evident natural variability in Nauru's shoreline that may be linked to factors such as ENSO, waves, tides and storm surges, the biggest shoreline changes between 1992 and 2020 occurred as episodic events due to anthropogenic interventions such as the building of ports or the runway extension. As such, the overall change in shoreline is not linear. A more detailed analysis using higher frequency shoreline change data (annual to sub-annual) should be undertaken to fully understand the climatic drivers affecting the shoreline in shorter time scales. To ensure that actionable information is provided to policy makers, an investigation into how rising sea levels will affect Nauru's shorelines in coming decades is advisable.

This study acts as a first indication of the current financial risk to Nauru due to coastal flooding. Coastal flooding is a compound event where tides, sea-level anomalies and waves all interact to create extreme total water levels nearshore. While tides and mean sea-level anomalies can be considered fairly homogeneous around Nauru (being a relatively small island nation), the wave climate varies significantly around the island. To improve the results of this study, we recommend future studies to downscale the wave conditions around Nauru using a regional wave model. The methodology could be further improved by using high-resolution numerical hydrodynamic and wave models (as opposed to an empirical approximation) to simulate the non-linear nearshore processes and inundation extent. However, for such work to be undertaken, appropriate nearshore bathymetry data would need to be collected.

The damage functions used in this study were obtained from PCRAFI (2013). The damage functions were tailored to damage from tsunamis and storm surges. To ensure consistency with previous work done in Nauru (e.g., GFDRR 2011) and to ensure compatibility with the available asset datasets, we used the same damage functions. However, for more accurate damage and loss information, future studies should consider developing tailored damage functions for wave-driven flooding.

To conclude, the results of this study quantify for the first time the annual expected loss due to wave-driven flooding in Nauru. Additionally, this study investigates the exacerbation of the loss due to sea-level rise. This will allow Nauru to plan and prioritize resources, investments, and further research to help prepare the nation for future increased sea levels.

References

Alberti, L., la Licata, I., Cantone M., 2017. Saltwater Intrusion and Freshwater Storage in Sand Sediments along the Coastline: Hydrogeological Investigations and Groundwater Modeling of Nauru Island. Water (Basel) 9, 788. https://doi.org/10.3390/w9100788

Allis, M., Williams, S., Wadwha, S., 2020. Coastal flooding from sea-level rise in Nauru: Stage 1-static inundation mapping. Hamilton.

Andrew, Neil L, Bright, P., de la Rua, L., Teoh, S.J., Vickers, M., 2019. Coastal proximity of populations in 22 Pacific Island Countries and Territories. PLoS One 14, e0223249. https://doi.org/10.1371/journal.pone.0223249

Australian Bureau of Meteorology, CSIRO, 2014. Climate Variability, Extremes and Change in the Western Tropical Pacific: New Science and Updated Country Reports 2014. Melbourne, Australia.

Australian Bureau of Meteorology, CSIRO, 2011. Climate change in the Pacific: Scientific Assessment and New Research. Volume 2: Country reports. [CSIRO Pub.], Melbourne, Australia.

Baldock, T.E., 2012. Dissipation of incident forced long waves in the surf zone—Implications for the concept of "bound" wave release at short wave breaking. Coastal Engineering 60, 276–285. https://doi.org/10.1016/j.coastaleng.2011.11.002

Becker, J.M., Merrifield, M.A., Ford, M., 2014. Water level effects on breaking wave setup for Pacific Island fringing reefs. Journal of Geophysical Research: Oceans 119, 914–932. https://doi.org/10.1002/2013JC009373

Beetham, E., Kench, P.S., 2018. Predicting wave overtopping thresholds on coral reef-island shorelines with future sea-level rise. Nature Communications 9, 1–8. https://doi.org/10.1038/s41467-018-06550-1

Beetham, E., Kench, P.S., Popinet, S., 2017. Future Reef Growth Can Mitigate Physical Impacts of Sea-Level Rise on Atoll Islands. Earth's Future 5, 1002–1014. https://doi.org/10.1002/2017EF000589

Bosserelle, C., Reddy, S., Lal, D., 2015. WACOP wave climate reports. Suva, Fiji Islands.

Burningham, H., Fernandez-Nunez, M., 2020. Shoreline change analysis, in: Sandy Beach Morphodynamics. Elsevier, pp. 439–460. https://doi.org/10.1016/b978-0-08-102927-5.00019-9

Chand, S.S., L. McBride, J., Tory, K.J., Wheeler, M.C., Walsh, K.J.E., 2013. Impact of Different ENSO Regimes on Southwest Pacific Tropical Cyclones. Journal of Climate 26, 600–608. https://doi.org/10.1175/JCLI-D-12-00114.1

Chand, S.S., Walsh, K.J.E., 2009. Tropical cyclone activity in the Fiji region: Spatial patterns and relationship to large-scale circulation. Journal of Climate 22, 3877–3893. https://doi.org/10.1175/2009JCLI2880.1

CSIRO, Australian Bureau of Meteorology, SPREP, 2015. Climate in the Pacific: A regional summary of new science and management tools, Pacific-Australia Climate Change Science and Adaptation Planning Program Summary Report. Commonwealth Scientific and Industrial Research Organisation, Melbourne, Australia.

Durrant, T., Greenslade, D., Hemar, M., Trenham, C., 2014. A Global Hindcast focussed on the Central and South Pacific, CAWCR Technical Report No. 070.

Fraser, S., Douglas, J., Simpson, A., Kuijper, M., Winsemius, H., Burzel, A., Hohmann, A., Taillefer, N., Giraud, P., ThinkHazard, C., 2017. ThinkHazard! Methodology report. Updated for ThinkHazard! Version 2.

Genz, A.S., Fletcher, C.H., Dunn, R.A., Frazer, L.N., Rooney, J.J., 2007. The Predictive Accuracy of Shoreline Change Rate Methods and Alongshore Beach Variation on Maui, Hawaii. Journal of Coastal Research 231, 87–105. https://doi.org/10.2112/05-0521.1

GFDRR, 2011. Pacific Catastrophe Risk Assessment and Financing Initiative, Country Risk Profile: Nauru.

He, C., 2000. Coastal erosion monitoring and advise on response strategies, Nauru. Suva, Fiji.

Hoeke, Ron K., Damlamian, H., Aucan, J., Wandres, M., 2021. Severe Flooding in the Atoll Nations of Tuvalu and Kiribati Triggered by a Distant Tropical Cyclone Pam. Front Mar Sci 7. https://doi.org/10.3389/fmars.2020.539646

Hoeke, R.K., McInnes, K.L., Kruger, J.C., McNaught, R.J., Hunter, J.R., Smithers, S.G., 2013. Widespread inundation of Pacific islands triggered by distant-source wind-waves. Global and Planetary Change 108, 128–138. https://doi.org/10.1016/j.gloplacha.2013.06.006

Humanitarian OpenStreetMap Team, 2020. Hot Export Tool [WWW Document]. https://export.hotosm.org/en/v3/.

IPCC, 2021. Summary for Policymakers, in: v. Masson-Delmotte, P. Zhai, A. Pirani, S.L. Connors, C. Péan, S. Berger, N. Caud, Y. Chen, L. Goldfarb, M.I. Gomis, M. Huang, K. Leitzell, E. Lonnoy, J.B.R. Matthews, T.K. Maycock, T. Waterfield, O. Yelekçi, R. Yu, B. Zhou (Eds.), Climate Change 2021: The Physical Science Basis. Contribution of Working Group I to the Sixth Assessment Report of the Intergovernmental Panel on Climate Change.

Jackson, C.W., Alexander, C.R., Bush, D.M., 2012. Application of the AMBUR R package for spatio-temporal analysis of shoreline change: Jekyll Island, Georgia, USA. Computers and Geosciences 41, 199–207. https://doi.org/10.1016/j.cageo.2011.08.009

Maharaj, R.J., 2000. Pacific islands at risk: Foreshore development and their vulnerability and implication for adaptation strategies to climate change. Suva, Fiji.

Merrifield, M.A., Becker, J.M., Ford, M., Yao, Y., 2014. Observations and estimates of wave-driven water level extremes at the Marshall Islands. Geophysical Research Letters 41, 7245–7253. https://doi.org/10.1002/2014GL061005

Muis, S., Verlaan, M., Winsemius, H.C., Aerts, J.C.J.H., Ward, P.J., 2016. A global reanalysis of storm surges and extreme sea levels. Nature Communications 7, 11969. https://doi.org/10.1038/ncomms11969

Pacific Catastrophe Risk Assessment & Financing Initiative (PCRAFI), 2013. Pacific Catastrophe Risk Assessment & Financing Initiative (PCRAFI) Risk Assessment - Summary Report. Washington DC, USA.

Paulik, R., Horspool, N., Woods, R., Griiths, N., Beale, T., Magill, C., Wild, A., Popovich Moffat, B., Glenn Walbran, N., Garlick, R., Griffiths, N., Popovich, B., Walbran, G., n.d. RiskScape: A exible multi-hazard risk modelling engine. https://doi.org/10.21203/rs.3.rs-1123016/v1

Perry, C.T., Alvarez-Filip, L., Graham, N.A.J., Mumby, P.J., Wilson, S.K., Kench, P.S., Manzello, D.P., Morgan, K.M., Slangen, A.B.A., Thomson, D.P., Januchowski-Hartley, F., Smithers, S.G., Steneck, R.S., Carlton, R., Edinger, E.N., Enochs, I.C., Estrada-Saldívar, N., Haywood, M.D.E., Kolodziej, G., Murphy, G.N., Pérez-Cervantes, E., Suchley, A., Valentino, L., Boenish, R., Wilson, M., Macdonald, C., 2018. Loss of coral reef growth capacity to track future increases in sea level. Nature 558, 396–400. https://doi.org/10.1038/s41586-018-0194-z

Pollock, N.J., 2014. Nauru Phosphate History and the Resource Curse Narrative. Journal de la société des océanistes 138–139, 107–120. https://doi.org/10.4000/jso.7055

Pomeroy, A., Lowe, R., Symonds, G., van Dongeren, A., Moore, C., 2012. The dynamics of infragravity wave transformation over a fringing reef. Journal of Geophysical Research: Oceans 117, 1–17. https://doi.org/10.1029/2012JC008310

Republic of Nauru, 2014. Second National Communication.

Smith, G., Juria, N., 2019. Diagnosis of historical inundation events in the Marshall Islands to assist early warning systems. Natural Hazards 99, 189–216. https://doi.org/10.1007/s11069-019-03735-9

Storlazzi, C.D., Gingerich, S.B., van Dongeren, A., Cheriton, O.M., Swarzenski, P.W., Quataert, E., Voss, C.I., Field, D.W., Annamalai, H., Piniak, G.A., McCall, R., 2018. Most atolls will be uninhabitable by the mid-21st century because of sea-level rise exacerbating wave-driven flooding. Science Advances 4, 1–10. https://doi.org/10.1126/sciadv.aap9741

Terry, J.P., Lau, A.Y.A., 2018. Magnitudes of nearshore waves generated by tropical cyclone Winston, the strongest landfalling cyclone in South Pacific records. Unprecedented or unremarkable? Sedimentary Geology 364, 276–285. https://doi.org/10.1016/j.sedgeo.2017.10.009

Thaman, R.R., 1992. Vegetation of Nauru and the Gilbert Islands: Case Studies of Poverty, Degradation, Disturbance, and Displacement! Pacific Science 46, 128–158.

The World Bank Group, 2021. Climate Risk Country Profile: Nauru.

Tuck, M.E., Ford, M.R., Masselink, G., Kench, P.S., 2019. Geomorphology Physical modelling of reef island topographic response to rising sea levels. Geomorphology 345, 106833. https://doi.org/10.1016/j.geomorph.2019.106833

Vetter, O., Becker, J.M., Merrifield, M.A., Pequignet, A.C., Aucan, J., Boc, S.J., Pollock, C.E., 2010. Wave setup over a Pacific Island fringing reef. Journal of Geophysical Research: Oceans 115, C12066. https://doi.org/10.1029/2010JC006455

Wandres, M., Aucan, J., Espejo, A., Jackson, N., de Ramon N'Yeurt, A., Damlamian, H., 2020. Distant-Source Swells Cause Coastal Inundation on Fiji's Coral Coast. Front Mar Sci 7, 1–10. https://doi.org/10.3389/fmars.2020.00546

Webb, A.P., Kench, P.S., 2010. The dynamic response of reef islands to sea-level rise: Evidence from multi-decadal analysis of island change in the Central Pacific. Global and Planetary Change 72, 234–246. https://doi.org/10.1016/j.gloplacha.2010.05.003

World Bank Group, 2022. Population, total - Nauru [WWW Document]. https://data.worldbank.org/indicator/SP.POP.TOTL?locations=NR.

Annex 1: RiskScape models and functions

[project]
description = Nauru pre-feasibility inundation risk assessment
auto-import = true

[bookmark Building_Nauru(exposure-layer)]
description = Buildings in Nauru, based on polygon (Source: Open Street Maps)
location = data/nauru_buildings_osm_2020.shp
crs-name = EPSG:32758

[bookmark PACRIS_Building_Nauru(exposure-layer)]
description = Buildings in Nauru (Source: PACRIS)
location = data/nauru_buildings_pacris_2012.shp
crs-name = EPSG:32758

[bookmark Roads_Nauru(exposure-layer)]
description = Roads in Nauru, line (Source: Open Street Maps)
location = data/nauru_roads_2020.shp
crs-name = EPSG:32758

[bookmark Population_Nauru(exposure-layer)]
description = Population gridded data for Nauru (resolution: 111m)
location = data/nauru_population_grid_2020.tif
crs-name = EPSG:32758

[bookmark Districts_Nauru(area-layer)]
description = Nauru districts (Source: Open Street Maps)
location = data/nauru_districts_2020.shp
crs-name = EPSG:32758

[bookmark Coastal_inundation(hazard-layer)]
description = Coastal inundation depth for Nauru with ARI (resolution: 5m)
location = data/SLR_SSP5-8.5_2100/500_ARI_SSP5-8.5H+_2100.tif
crs-name = EPSG:32758

[function building_damage]

description = A function to assess economic damage to buildings due to flood

location = functions/damageBuildingsDDF_stormsurge.py

argument-types = [building: struct(the_geom: geometry, Const: text, Value: floating), hazard_depth: nullable(floating)]

return-type = struct(Exposed: integer, Loss: nullable(floating), yval: nullable(floating))

framework = cpython

[model exposed-buildings-by-district-2020]

framework = wizard

version = 1.0.0-wizard-v1

description = Produces the amount of buildings exposed to coastal inundation per district in csv output

input-exposures.layer = Building_Nauru(exposure-layer)

input-exposures.geoprocess = false

input-hazards.layer = Coastal_inundation(hazard-layer)

input-areas.layer = Districts_Nauru(area-layer)

input-areas.geoprocess = false

sample.hazards-by = CLOSEST

analysis.function = is_exposed

report-event-impact.group-by[0] = area.name as Districts

report-event-impact.group-by[1] = consequence as consequence

report-event-impact.aggregate[0] = count(exposure.Osm_ID_1) as Exposed_Buildings

report-event-impact.sort-by[0][attribute] = Districts

report-event-impact.sort-by[0][direction] = ASC

report-event-impact.format = csv

[model exposed-population]

framework = wizard

version = 1.0.0-wizard-v1

description = Produces the population exposed to coastal inundation per district in csv output

input-exposures.layer = Population_Nauru(exposure-layer)

input-exposures.geoprocess = false

input-hazards.layer = Coastal_inundation(hazard-layer)

input-areas.layer = Districts_Nauru(area-layer)

input-areas.geoprocess = false

sample.hazards-by = CLOSEST

sample.hazards-buffer = 77

sample.areas-buffer = 120
analysis.function = is_exposed
report-event-impact.group-by[0] = area.name as Districts
report-event-impact.group-by[1] = consequence as consequence
report-event-impact.aggregate[0] = sum(exposure.value) as Exposed_population
report-event-impact.sort-by[0][attribute] = Districts
report-event-impact.sort-by[0][direction] = ASC
report-event-impact.format = csv
reports.name[0] = Exposed_population
report-Exposed_population.format = shapefile

[model exposed-road-length]
framework = wizard
version = 1.0.0-wizard-v1
description = Produces the road length exposed to coastal inundation per district in csv output
input-exposures.layer = Roads_Nauru(exposure-layer)
input-exposures.geoprocess = true
input-exposures.cut = BY_DISTANCE
input-exposures.cut-distance = 5
input-exposures.recompute[0][expression] = measure(exposure)
input-exposures.recompute[0][attribute] = exposure.Rd_length
input-exposures.save-raw-results = true
input-hazards.layer = Coastal_inundation(hazard-layer)
input-areas.layer = Districts_Nauru(area-layer)
input-areas.geoprocess = false
sample.hazards-by = CLOSEST
analysis.function = is_exposed
report-event-impact.filter = consequence = 1
report-event-impact.group-by[0] = area.name as Districts
report-event-impact.aggregate[0] = sum(exposure.Rd_length) as Exposed_road_length
report-event-impact.sort-by[0][attribute] = Districts
report-event-impact.sort-by[0][direction] = ASC
report-event-impact.format = csv

[model exposed-buildings-by-district-2012]

framework = wizard

version = 1.0.0-wizard-v1

description = Produces the amount of buildings exposed to coastal inundation per district in csv output for 2012 PACRIS data

input-exposures.layer = PACRIS_Building_Nauru(exposure-layer)

input-exposures.geoprocess = true

input-exposures.enlarge = true

input-exposures.enlarge-by[mode] = ROUND

input-exposures.enlarge-by[remove-overlaps] = true

input-exposures.enlarge-by[distance] = 5

input-hazards.layer = Coastal_inundation(hazard-layer)

input-areas.layer = Districts_Nauru(area-layer)

input-areas.geoprocess = false

sample.hazards-by = CLOSEST

sample.areas-buffer = 10

analysis.function = is_exposed

report-event-impact.group-by[0] = area.name as Districts

report-event-impact.group-by[1] = consequence as consequence

report-event-impact.aggregate[0] = count(exposure.ID) as Exposed_Buildings

report-event-impact.sort-by[0][attribute] = Districts

report-event-impact.sort-by[0][direction] = ASC

report-event-impact.format = csv

Annex 2: RiskScape model incorporating the fragility functions

The fragility functions were obtained from the Pacific Catastrophe Risk Assessment & Financing Initiative (PCRAFI 2013), which provides building damage percentages associated with storm surge and tsunami inundation heights. The mean of these two damage states were determined to be conservative as the damage state for storm surge flooding is quite low.

Building damage state is provided for storm surges, tsunamis, and the mean of both in relation to inundation heights of 0 m, 0.5 m, 1 m, 2 m, 3 m, 4 m, and 5 m.

Construction type	Building damage state in relation to inundation heights of: [0 m, 0.5 m, 1 m, 2 m, 3 m, 4 m, 5 m]		
	Storm surge	Tsunami	Mean
Multi-story combination masonry/ concrete & timber frame	[0, 0.0005, 0.005, 0.0735, 0.128, 0.128, 0.128]	[0, 0, 0.1364, 0.2273, 0.3364, 0.5182, 0.7]	[0, 0.00025, 0.0707, 0.1504, 0.2322, 0.3231, 0.414]
Multi-story masonry/concrete	[0, 0, 0, 0.04, 0.09, 0.09, 0.09]	[0, 0, 0.1364, 0.2273, 0.3364, 0.5182, 0.7]	[0, 0, 0.0682, 0.1337, 0.2132, 0.3041, 0.395]
Multi-story steel frame	[0, 0, 0, 0.0408, 0.0918, 0.0918, 0.0918]	[0, 0, 0.1364, 0.2273, 0.3364, 0.5182, 0.7]	[0, 0, 0.0682, 0.1341, 0.2141, 0.305, 0.3959]
Multi-story timber frame with closed-under	[0, 0.005, 0.05, 0.375, 0.47, 0.47, 0.47]	[0, 0.12, 0.22, 0.54, 0.82, 0.96, 1]	[0, 0.063, 0.135, 0.458, 0.645, 0.715, 0.735]
Multi-story timber frame with open-under	[0, 0.005, 0.05, 0.375, 0.47, 0.47, 0.47]	[0, 0.12, 0.22, 0.54, 0.82, 0.96, 1]	[0, 0.063, 0.135, 0.458, 0.645, 0.715, 0.735]
Open-walled structure with non-wooden pole frame	[0, 0, 0, 0.0816, 0.1836, 0.1836, 0.1836]	[0, 0, 0.1364, 0.2273, 0.3364, 0.5182, 0.7]	[0, 0, 0.0682, 0.1545, 0.26, 0.3509, 0.4418]
Open-walled structure with wooden pole frame (Fale)	[0, 0, 0, 0.0816, 0.1836, 0.1836, 0.1836]	[0, 0, 0.1364, 0.2273, 0.3364, 0.5182, 0.7]	[0, 0, 0.0682, 0.1545, 0.26, 0.3509, 0.4418]
Other multi-story	[0, 0.0004, 0.004, 0.0588, 0.1024, 0.1024, 0.1024]	[0, 0.12, 0.22, 0.54, 0.82, 0.96, 1]	[0, 0.0602, 0.112, 0.2994, 0.4612, 0.5312, 0.5512]
Other single story	[0,0.0008, 0.008, 0.1176, 0.2048, 0.2048, 0.2048]	[0, 0.25, 0.7, 0.975, 1, 1, 1]	[0, 0.1254, 0.354, 0.5463, 0.6024, 0.6024, 0.6024]
Single story combination masonry/ concrete & timber frame	[0, 0.001, 0.01, 0.147, 0.256, 0.256, 0.256]	[0, 0.12, 0.22, 0.54, 0.82, 0.96, 1]	[0, 0.0605, 0.115, 0.3435, 0.538, 0.608, 0.628]
Single story masonry/concrete	[0, 0, 0, 0.08, 0.18, 0.18, 0.18]	[0, 0.12, 0.22, 0.54, 0.82, 0.96, 1]	[0, 0.06, 0.11, 0.31, 0.5, 0.57, 0.59]
Single story steel frame	[0, 0, 0, 0.0816, 0.1836, 0.1836, 0.1836]	[0, 0, 0.1364, 0.2273, 0.3364, 0.5182, 0.7]	[0, 0, 0.0682, 0.1545, 0.26, 0.3509, 0.4418]
Single story timber frame	[0, 0.01, 0.1, 0.75, 0.94, 0.94, 0.94]	[0, 0.25, 0.7, 0.975, 1, 1, 1]	[0, 0.13, 0.4, 0.863, 0.97, 0.97, 0.97]
Traditional	[0, 0.008, 0.08, 0.6, 0.752, 0.752, 0.752]	[0, 0.25, 0.7, 0.975, 1, 1, 1]	[0, 0.129, 0.39, 0.7875, 0.876, 0.876, 0.876]
Uninhabitable or poor construction	[0, 0.01, 0.1, 0.75, 0.94, 0.94, 0.94]	[0, 0.25, 0.7, 0.975, 1, 1, 1]	[0, 0.13, 0.4, 0.863, 0.97, 0.97, 0.97]

Annex 3: Number of buildings exposed per district using OSM 2020 building data

Projections	ARI	Aiwo	Anabar	Anetan	Anibare	Baitsi	Boe	Buada	Denigomodu	Ewa	Ijuw	Meneng	Nibok	Uaboe	Yaren	Total
Present	5	1	68	26	20	1	8	0	0	28	10	88	0	4	15	269
	10	1	75	29	21	1	10	0	0	34	11	94	0	5	16	297
	25	1	85	35	24	3	14	0	0	41	12	99	0	6	18	338
	50	2	89	40	24	3	19	0	0	45	13	106	1	8	19	369
	100	2	99	43	23	3	21	0	0	48	16	111	1	9	19	395
	250	4	112	48	22	6	23	0	0	52	18	119	1	11	20	436
	500	5	117	53	21	9	23	0	0	56	21	123	7	12	20	467
SSP1-1.9 (2050)	5	1	85	34	29	1	13	0	0	38	15	138	0	5	19	378
	10	2	90	37	31	3	19	0	0	42	17	150	0	7	20	418
	25	2	102	43	32	3	21	0	0	47	20	164	1	9	20	464
	50	3	110	46	32	4	23	0	0	48	22	172	1	9	20	490
	100	5	115	50	32	6	23	0	0	52	24	175	1	11	20	514
	250	5	127	56	32	10	25	0	0	56	26	177	10	14	22	560
	500	11	134	68	31	17	31	0	0	65	26	180	13	21	23	620
SSP1-1.9 (2100)	5	3	110	45	35	3	23	0	0	47	26	192	1	9	27	521
	10	3	117	47	36	4	24	0	0	48	26	200	1	9	31	546
	25	5	126	51	36	6	26	0	0	51	28	206	1	12	43	591
	50	5	132	53	36	9	31	0	0	53	30	211	6	13	52	631
	100	7	139	65	36	14	40	0	0	56	31	213	12	19	57	689
	250	17	157	78	36	19	47	0	0	75	33	214	18	24	62	780
	500	38	165	87	36	29	53	0	3	97	34	214	25	29	68	878
SSP5-8.5 (2050)	5	2	86	35	31	3	15	0	0	39	16	147	0	6	20	400
	10	2	95	40	33	3	21	0	0	42	19	160	1	8	20	444
	25	3	106	45	33	3	21	0	0	48	22	175	1	9	20	486
	50	3	112	46	33	4	23	0	0	49	24	179	1	9	21	504
	100	5	119	51	33	7	24	0	0	52	26	182	1	12	24	536
	250	7	129	64	33	13	28	0	0	56	26	184	12	16	26	594
	500	12	139	71	32	19	34	0	0	71	28	185	14	24	26	655

Projections	ARI	Aiwo	Anabar	Anetan	Anibare	Baitsi	Boe	Buada	Denigomodu	Ewa	Ijuw	Meneng	Nibok	Uaboe	Yaren	Total
SSP5-8.5 (2100)	5	5	141	53	46	9	39	0	0	53	33	236	4	13	87	719
	10	7	150	64	49	13	43	0	0	54	35	242	12	19	97	785
	25	14	164	70	51	17	50	0	0	59	35	252	13	24	104	853
	50	29	171	84	53	22	55	0	0	71	37	254	20	24	112	932
	100	42	181	87	55	29	63	0	3	90	41	257	26	29	117	1020
	250	59	195	113	53	36	72	0	3	111	45	258	36	39	122	1142
	500	74	211	145	51	45	78	0	7	128	49	259	45	49	122	1263

6.

Annex 4: Percentage of buildings exposed per district using OSM 2020 building data

Projections	ARI	Aiwo	Anabar	Anetan	Anibare	Baitsi	Boe	Buada	Denigomodu	Ewa	Ijuw	Meneng	Nibok	Uaboe	Yaren	Total
Present	5	0.2%	21.5%	10.1%	9.6%	0.6%	3.7%	0.0%	0.0%	7.1%	5.0%	13.3%	0.0%	3.6%	4.6%	6.2%
	10	0.2%	23.7%	11.3%	10.1%	0.6%	4.6%	0.0%	0.0%	8.7%	5.5%	14.2%	0.0%	4.5%	4.9%	6.9%
	25	0.2%	26.9%	13.6%	11.5%	1.9%	6.5%	0.0%	0.0%	10.4%	6.0%	15.0%	0.0%	5.5%	5.5%	7.8%
	50	0.4%	28.2%	15.6%	11.5%	1.9%	8.8%	0.0%	0.0%	11.5%	6.5%	16.1%	0.4%	7.3%	5.8%	8.6%
	100	0.4%	31.3%	16.7%	11.1%	1.9%	9.7%	0.0%	0.0%	12.2%	8.0%	16.8%	0.4%	8.2%	5.8%	9.2%
	250	0.7%	35.4%	18.7%	10.6%	3.8%	10.6%	0.0%	0.0%	13.2%	9.0%	18.0%	0.4%	10.0%	6.1%	10.1%
	500	0.9%	37.0%	20.6%	10.1%	5.7%	10.6%	0.0%	0.0%	14.2%	10.5%	18.6%	3.1%	10.9%	6.1%	10.8%
SSP1-1.9 (2050)	5	0.2%	26.9%	13.2%	13.9%	0.6%	6.0%	0.0%	0.0%	9.7%	7.5%	20.9%	0.0%	4.5%	5.8%	8.8%
	10	0.4%	28.5%	14.4%	14.9%	1.9%	8.8%	0.0%	0.0%	10.7%	8.5%	22.7%	0.0%	6.4%	6.1%	9.7%
	25	0.4%	32.3%	16.7%	15.4%	1.9%	9.7%	0.0%	0.0%	12.0%	10.0%	24.8%	0.4%	8.2%	6.1%	10.8%
	50	0.5%	34.8%	17.9%	15.4%	2.5%	10.6%	0.0%	0.0%	12.2%	11.0%	26.1%	0.4%	8.2%	6.1%	11.4%
	100	0.9%	36.4%	19.5%	15.4%	3.8%	10.6%	0.0%	0.0%	13.2%	12.0%	26.5%	0.4%	10.0%	6.1%	11.9%
	250	0.9%	40.2%	21.8%	15.4%	6.3%	11.5%	0.0%	0.0%	14.2%	13.0%	26.8%	4.4%	12.7%	6.7%	13.0%
	500	1.9%	42.4%	26.5%	14.9%	10.8%	14.3%	0.0%	0.0%	16.5%	13.0%	27.3%	5.8%	19.1%	7.0%	14.4%
SSP1-1.9 (2100)	5	0.5%	34.8%	17.5%	16.8%	1.9%	10.6%	0.0%	0.0%	12.0%	13.0%	29.1%	0.4%	8.2%	8.2%	12.1%
	10	0.5%	37.0%	18.3%	17.3%	2.5%	11.1%	0.0%	0.0%	12.2%	13.0%	30.3%	0.4%	8.2%	9.4%	12.7%
	25	0.9%	39.9%	19.8%	17.3%	3.8%	12.0%	0.0%	0.0%	13.0%	14.0%	31.2%	0.4%	10.9%	13.1%	13.7%
	50	0.9%	41.8%	20.6%	17.3%	5.7%	14.3%	0.0%	0.0%	13.5%	15.0%	32.0%	2.7%	11.8%	15.8%	14.6%
	100	1.2%	44.0%	25.3%	17.3%	8.9%	18.4%	0.0%	0.0%	14.2%	15.5%	32.3%	5.3%	17.3%	17.3%	16.0%
	250	3.0%	49.7%	30.4%	17.3%	12.0%	21.7%	0.0%	0.0%	19.1%	16.5%	32.4%	8.0%	21.8%	18.8%	18.1%
	500	6.7%	52.2%	33.9%	17.3%	18.4%	24.4%	0.0%	0.8%	24.7%	17.0%	32.4%	11.1%	26.4%	20.7%	20.4%
SSP5-8.5 (2050)	5	0.4%	27.2%	13.6%	14.9%	1.9%	6.9%	0.0%	0.0%	9.9%	8.0%	22.3%	0.0%	5.5%	6.1%	9.3%
	10	0.4%	30.1%	15.6%	15.9%	1.9%	9.7%	0.0%	0.0%	10.7%	9.5%	24.2%	0.4%	7.3%	6.1%	10.3%
	25	0.5%	33.5%	17.5%	15.9%	1.9%	9.7%	0.0%	0.0%	12.2%	11.0%	26.5%	0.4%	8.2%	6.1%	11.3%
	50	0.5%	35.4%	17.9%	15.9%	2.5%	10.6%	0.0%	0.0%	12.5%	12.0%	27.1%	0.4%	8.2%	6.4%	11.7%
	100	0.9%	37.7%	19.8%	15.9%	4.4%	11.1%	0.0%	0.0%	13.2%	13.0%	27.6%	0.4%	10.9%	7.3%	12.4%
	250	1.2%	40.8%	24.9%	15.9%	8.2%	12.9%	0.0%	0.0%	14.2%	13.0%	27.9%	5.3%	14.5%	7.9%	13.8%
	500	2.1%	44.0%	27.6%	15.4%	12.0%	15.7%	0.0%	0.0%	18.1%	14.0%	28.0%	6.2%	21.8%	7.9%	15.2%

Projections	ARI	Aiwo	Anabar	Anetan	Anibare	Baitsi	Boe	Buada	Denigomodu	Ewa	Ijuw	Meneng	Nibok	Uaboe	Yaren	Total
SSP5-8.5 (2100)	5	0.9%	44.6%	20.6%	22.1%	5.7%	18.0%	0.0%	0.0%	13.5%	16.5%	35.8%	1.8%	11.8%	26.4%	16.7%
	10	1.2%	47.5%	24.9%	23.6%	8.2%	19.8%	0.0%	0.0%	13.7%	17.5%	36.7%	5.3%	17.3%	29.5%	18.2%
	25	2.5%	51.9%	27.2%	24.5%	10.8%	23.0%	0.0%	0.0%	15.0%	17.5%	38.2%	5.8%	21.8%	31.6%	19.8%
	50	5.1%	54.1%	32.7%	25.5%	13.9%	25.3%	0.0%	0.0%	18.1%	18.5%	38.5%	8.9%	21.8%	34.0%	21.6%
	100	7.4%	57.3%	33.9%	26.4%	18.4%	29.0%	0.0%	0.8%	22.9%	20.5%	38.9%	11.6%	26.4%	35.6%	23.6%
	250	10.4%	61.7%	44.0%	25.5%	22.8%	33.2%	0.0%	0.8%	28.2%	22.5%	39.1%	16.0%	35.5%	37.1%	26.5%
	500	13.1%	66.8%	56.4%	24.5%	28.5%	35.9%	0.0%	1.8%	32.6%	24.5%	39.2%	20.0%	44.5%	37.1%	29.3%

Annex 5: Number of people exposed per district using SPC Statistics 2020 population data

Projections	ARI	Aiwo	Anabar	Anetan	Anibare	Baitsi	Boe	Buada	Denigomodu	Ewa	Ijuw	Meneng	Nibok	Uaboe	Yaren	Total
Present	5	177	342	207	217	407	736	0	121	494	173	1246	250	307	406	5083
	10	177	342	207	217	407	736	0	121	494	173	1246	250	307	406	5083
	25	177	342	207	217	412	818	0	259	494	173	1317	264	307	406	5393
	50	177	342	207	217	475	861	0	259	494	173	1317	330	307	406	5565
	100	460	342	207	217	482	861	0	259	494	173	1317	461	310	406	5989
	250	460	342	207	217	572	861	0	259	529	173	1317	461	310	490	6198
	500	460	342	207	217	572	861	0	359	529	173	1317	534	350	490	6411
SSP1-1.9 (2050)	5	177	342	207	220	407	736	0	121	494	173	1317	250	307	406	5157
	10	177	342	207	220	475	861	0	259	494	173	1317	286	307	490	5608
	25	363	342	207	220	482	861	0	259	494	173	1317	377	310	490	5895
	50	460	342	207	220	482	861	0	259	494	173	1317	461	310	511	6097
	100	460	342	207	220	572	861	0	259	529	173	1338	467	310	511	6249
	250	521	435	207	220	572	861	0	359	529	173	1338	534	350	532	6631
	500	563	435	207	220	572	861	0	413	529	173	1338	534	350	532	6727
SSP1-1.9 (2100)	5	363	342	207	220	482	861	0	259	494	173	1338	418	310	532	5999
	10	460	342	207	220	482	861	0	259	494	173	1338	461	310	532	6139
	25	460	435	207	220	572	861	0	326	529	173	1338	534	310	547	6512
	50	460	435	207	220	572	861	0	326	529	173	1338	534	350	547	6552
	100	521	435	207	220	572	861	0	359	529	173	1338	534	350	547	6646
	250	798	435	207	220	572	861	0	413	529	173	1338	544	391	547	7028
	500	798	435	207	220	572	861	0	413	529	173	1338	544	391	562	7043
SSP5-8.5 (2050)	5	177	342	207	220	412	818	0	121	494	173	1317	264	307	490	5342
	10	177	342	207	220	475	861	0	259	494	173	1317	286	307	490	5608
	25	460	342	207	220	482	861	0	259	494	173	1338	461	310	511	6118
	50	460	342	207	220	482	861	0	259	494	173	1338	461	310	511	6118
	100	460	435	207	220	572	861	0	326	529	173	1338	534	310	532	6497
	250	521	435	207	220	572	861	0	359	529	173	1338	534	350	532	6631
	500	563	435	207	220	572	861	0	413	529	173	1338	534	350	532	6727

Projections	ARI	Aiwo	Anabar	Anetan	Anibare	Baitsi	Boe	Buada	Denigomodu	Ewa	Ijuw	Meneng	Nibok	Uaboe	Yaren	Total
SSP5-8.5 (2100)	5	460	435	207	220	572	861	0	326	529	173	1338	534	350	562	6567
	10	521	435	207	220	572	861	0	326	529	173	1338	534	350	562	6628
	25	706	435	207	220	572	861	0	359	529	173	1338	544	350	592	6886
	50	798	435	207	220	572	861	0	413	529	173	1338	544	391	592	7073
	100	798	435	207	220	572	950	0	413	529	173	1338	544	391	592	7162
	250	798	435	207	220	608	950	0	436	529	173	1338	544	391	592	7221
	500	880	435	207	220	608	950	0	521	529	173	1338	544	391	592	7388

Annex 6: Percentage of population exposed per district using SPC Statistics 2020 population data

Projections	ARI	Aiwo	Anabar	Anetan	Anibare	Baitsi	Boe	Buada	Denigomodu	Ewa	Ijuw	Meneng	Nibok	Uaboe	Yaren	Total
Present	5	11%	79%	100%	83%	63%	60%	0%	6%	93%	86%	86%	45%	79%	58%	46%
	10	11%	79%	100%	83%	63%	60%	0%	6%	93%	86%	86%	45%	79%	58%	46%
	25	11%	79%	100%	83%	64%	67%	0%	14%	93%	86%	91%	48%	79%	58%	48%
	50	11%	79%	100%	83%	74%	71%	0%	14%	93%	86%	91%	60%	79%	58%	50%
	100	29%	79%	100%	83%	75%	71%	0%	14%	93%	86%	91%	83%	79%	58%	54%
	250	29%	79%	100%	83%	89%	71%	0%	14%	100%	86%	91%	83%	79%	70%	56%
	500	29%	79%	100%	83%	89%	71%	0%	19%	100%	86%	91%	96%	90%	70%	58%
SSP1-1.9 (2050)	5	11%	79%	100%	84%	63%	60%	0%	6%	93%	86%	91%	45%	79%	58%	46%
	10	11%	79%	100%	84%	74%	71%	0%	14%	93%	86%	91%	52%	79%	70%	50%
	25	23%	79%	100%	84%	75%	71%	0%	14%	93%	86%	91%	68%	79%	70%	53%
	50	29%	79%	100%	84%	75%	71%	0%	14%	93%	86%	91%	83%	79%	73%	55%
	100	29%	79%	100%	84%	89%	71%	0%	14%	100%	86%	93%	84%	79%	73%	56%
	250	33%	100%	100%	84%	89%	71%	0%	19%	100%	86%	93%	96%	90%	76%	60%
	500	36%	100%	100%	84%	89%	71%	0%	22%	100%	86%	93%	96%	90%	76%	60%
SSP1-1.9 (2100)	5	23%	79%	100%	84%	75%	71%	0%	14%	93%	86%	93%	75%	79%	76%	54%
	10	29%	79%	100%	84%	75%	71%	0%	14%	93%	86%	93%	83%	79%	76%	55%
	25	29%	100%	100%	84%	89%	71%	0%	17%	100%	86%	93%	96%	79%	78%	58%
	50	29%	100%	100%	84%	89%	71%	0%	17%	100%	86%	93%	96%	90%	78%	59%
	100	33%	100%	100%	84%	89%	71%	0%	19%	100%	86%	93%	96%	90%	78%	60%
	250	51%	100%	100%	84%	89%	71%	0%	22%	100%	86%	93%	98%	100%	78%	63%
	500	51%	100%	100%	84%	89%	71%	0%	22%	100%	86%	93%	98%	100%	80%	63%
SSP5-8.5 (2050)	5	11%	79%	100%	84%	64%	67%	0%	6%	93%	86%	91%	48%	79%	70%	48%
	10	11%	79%	100%	84%	74%	71%	0%	14%	93%	86%	91%	52%	79%	70%	50%
	25	29%	79%	100%	84%	75%	71%	0%	14%	93%	86%	93%	83%	79%	73%	55%
	50	29%	79%	100%	84%	75%	71%	0%	14%	93%	86%	93%	83%	79%	73%	55%
	100	29%	100%	100%	84%	89%	71%	0%	17%	100%	86%	93%	96%	79%	76%	58%
	250	33%	100%	100%	84%	89%	71%	0%	19%	100%	86%	93%	96%	90%	76%	60%
	500	36%	100%	100%	84%	89%	71%	0%	22%	100%	86%	93%	96%	90%	76%	60%

Projections	ARI	Aiwo	Anabar	Anetan	Anibare	Baitsi	Boe	Buada	Denigomodu	Ewa	Ijuw	Meneng	Nibok	Uaboe	Yaren	Total
SSP5-8.5 (2100)	5	29%	100%	100%	84%	89%	71%	0%	17%	100%	86%	93%	96%	90%	80%	59%
	10	33%	100%	100%	84%	89%	71%	0%	17%	100%	86%	93%	96%	90%	80%	59%
	25	45%	100%	100%	84%	89%	71%	0%	19%	100%	86%	93%	98%	90%	84%	62%
	50	51%	100%	100%	84%	89%	71%	0%	22%	100%	86%	93%	98%	100%	84%	63%
	100	51%	100%	100%	84%	89%	78%	0%	22%	100%	86%	93%	98%	100%	84%	64%
	250	51%	100%	100%	84%	94%	78%	0%	23%	100%	86%	93%	98%	100%	84%	65%
	500	56%	100%	100%	84%	94%	78%	0%	28%	100%	86%	93%	98%	100%	84%	66%

Annex 7: Road length exposed (in metres) per district using OSM 2020 road data

Projections	ARI	Aiwo	Anabar	Anetan	Anibare	Baitsi	Boe	Buada	Denigomodu	Ewa	Ijuw	Meneng	Nibok	Uaboe	Yaren	Total
Present	5	12	750	337	795	14	70	0	0	46	109	489	0	54	49	2725
	10	17	778	362	855	14	79	0	0	46	144	524	0	54	59	2932
	25	82	813	407	880	19	84	0	0	46	169	574	0	59	64	3197
	50	102	863	451	890	19	89	0	0	46	199	579	0	59	74	3371
	100	107	914	506	905	19	100	0	0	55	219	594	0	64	89	3572
	250	112	987	620	905	59	115	0	0	60	314	604	0	79	119	3974
	500	112	1037	730	880	117	140	0	0	125	344	609	0	84	119	4297
SSP1-1.9_2050	5	52	813	392	1145	19	84	0	0	46	194	680	0	59	89	3573
	10	97	873	436	1209	19	89	0	0	46	209	751	0	59	119	3907
	25	102	959	501	1249	19	105	0	0	50	294	911	0	64	124	4378
	50	107	977	585	1274	24	110	0	0	60	329	1040	0	79	139	4724
	100	112	1027	635	1274	59	140	0	0	60	364	1119	0	79	139	5008
	250	117	1187	775	1259	122	170	0	0	130	384	1234	0	99	139	5616
	500	172	1392	910	1244	172	200	0	0	256	424	1259	0	126	144	6299
SSP1-1.9_2100	5	102	987	530	1521	19	110	0	0	50	354	1589	0	64	159	5485
	10	107	1032	585	1551	24	135	0	0	60	384	1734	0	79	169	5860
	25	112	1172	665	1581	59	165	0	0	60	414	1877	0	79	212	6396
	50	117	1307	760	1596	122	190	0	0	65	434	1922	0	84	280	6877
	100	147	1442	835	1601	132	270	0	0	150	447	1962	0	114	330	7430
	250	227	1575	1015	1591	202	340	0	0	361	482	1977	0	174	345	8289
	500	417	1760	1225	1586	242	470	0	0	623	487	1982	0	234	395	9421
SSP5-8.5_2050	5	57	843	416	1229	19	89	0	0	46	204	726	0	59	119	3807
	10	97	893	451	1269	19	100	0	0	46	249	891	0	59	119	4193
	25	102	972	516	1289	19	110	0	0	50	319	1085	0	64	134	4660
	50	107	1007	595	1309	24	130	0	0	60	344	1219	0	79	139	5013
	100	112	1072	650	1314	59	145	0	0	60	379	1279	0	79	139	5288
	250	132	1272	790	1289	122	180	0	0	140	409	1359	0	104	169	5966
	500	182	1442	950	1284	187	245	0	0	301	434	1404	0	141	169	6739

Projections	ARI	Aiwo	Anabar	Anetan	Anibare	Baitsi	Boe	Buada	Denigomodu	Ewa	Ijuw	Meneng	Nibok	Uaboe	Yaren	Total
SSP5-8.5_2100	5	122	1417	750	1845	122	260	0	0	60	477	2271	0	84	697	8105
	10	137	1532	835	1895	127	310	0	0	90	507	2398	0	104	772	8707
	25	242	1675	935	1925	177	450	0	0	201	512	2493	0	146	841	9597
	50	342	1825	1045	1930	207	490	0	0	311	532	2573	0	204	926	10385
	100	536	2135	1225	1925	242	580	0	0	558	547	2620	0	234	989	11591
	250	767	2599	1508	1910	262	815	0	0	893	582	2660	12	296	1104	13408
	500	1044	2978	1968	1900	297	930	0	110	1143	602	2700	72	348	1225	15317

Annex 8: Number of buildings exposed per district using PACRIS 2012 building data

Projections	ARI	Aiwo	Anabar	Anetan	Anibare	Baitsi	Boe	Buada	Denigomodu	Ewa	Ijuw	Meneng	Nibok	Uaboe	Yaren	Total
Present	5	1	21	18	13	4	8	0	0	15	12	70	0	2	10	174
	10	1	21	20	14	5	10	0	0	17	12	74	0	4	11	189
	25	1	25	21	14	6	14	0	0	19	12	80	0	4	12	208
	50	1	25	21	14	6	14	0	0	22	13	87	0	6	12	221
	100	2	26	21	14	7	16	0	0	28	15	92	0	7	12	240
	250	3	27	24	14	8	21	0	0	29	17	96	1	8	12	260
	500	4	27	30	14	11	25	0	0	31	18	99	2	8	12	281
SSP1-1.9 (2050)	5	1	25	21	17	5	14	0	0	18	15	102	0	4	12	234
	10	1	25	21	18	6	15	0	0	22	16	113	0	5	12	254
	25	3	26	21	19	6	18	0	0	24	17	123	0	6	13	276
	50	3	27	24	19	8	22	0	0	29	18	127	1	8	13	299
	100	4	27	25	19	8	27	0	0	29	18	128	1	8	14	308
	250	5	27	31	19	11	28	0	0	31	18	129	3	10	16	328
	500	9	30	35	19	18	33	0	0	40	18	132	7	16	16	373
SSP1-1.9 (2100)	5	3	26	22	24	7	20	0	0	24	18	138	0	7	17	306
	10	3	27	24	25	8	27	0	0	29	18	140	1	8	19	329
	25	4	27	26	26	8	29	0	0	29	18	143	1	8	28	347
	50	4	27	29	26	11	33	0	0	29	19	147	2	9	31	367
	100	7	30	33	26	15	43	0	0	33	21	148	6	13	35	410
	250	16	33	37	26	23	50	0	0	46	21	149	9	21	38	469
	500	30	35	42	26	30	53	0	1	62	22	149	16	23	39	528
SSP5-8.5 (2050)	5	1	25	21	18	6	14	0	0	19	16	111	0	4	12	247
	10	1	26	21	19	6	16	0	0	22	17	122	0	6	13	269
	25	3	26	22	20	7	19	0	0	28	18	127	0	7	13	290
	50	3	27	24	21	8	24	0	0	29	18	129	1	8	14	306
	100	4	27	26	21	8	27	0	0	29	18	133	1	8	16	318
	250	6	27	32	20	14	29	0	0	33	18	134	4	10	16	343
	500	10	30	35	20	20	39	0	0	43	18	134	7	18	16	390

Projections	ARI	Aiwo	Anabar	Anetan	Anibare	Baitsi	Boe	Buada	Denigomodu	Ewa	Ijuw	Meneng	Nibok	Uaboe	Yaren	Total
SSP5-8.5 (2100)	5	4	30	29	37	11	44	0	0	29	22	165	1	9	52	433
	10	7	31	33	39	14	48	0	0	30	22	166	4	12	56	462
	25	13	35	35	39	19	51	0	0	36	24	169	7	18	61	507
	50	21	36	39	40	23	57	0	0	45	26	172	11	21	64	555
	100	31	41	43	39	29	62	0	1	56	26	172	16	24	68	608
	250	40	54	59	39	36	73	0	1	77	27	173	28	33	69	709
	500	46	61	80	39	42	77	0	3	83	27	174	34	35	71	772

Annex 9: Nauru building loss per fragility function

Projections	ARI	Building loss (USD 2012)		
		Mean fragility function	Storm surge fragility function	Tsunami fragility function
Present	5	2715763.30	566529.07	4865300.41
	10	3343832.98	811555.40	5877298.46
	25	4411564.39	1253470.40	7567530.34
	50	5384190.39	1790519.84	8977110.52
	100	6239141.52	2400027.43	10075158.75
	250	8308265.53	3766265.43	12842541.15
	500	9549945.70	4907950.41	14188757.23
SSP1-1.9 (2050)	5	4726361.60	1363777.05	8088353.19
	10	5898815.94	1901045.57	9894496.75
	25	7345769.27	2753372.49	11933469.48
	50	8387419.44	3419873.39	13349241.43
	100	9980397.65	4503168.34	15448834.57
	250	12061857.24	6135312.42	17979883.84
	500	13168856.82	7248784.76	19080701.23
SSP1-1.9 (2100)	5	9721282.00	3768879.48	15667925.13
	10	11137125.64	4566537.71	17706653.72
	25	13125910.44	5973862.78	20274099.77
	50	14910995.85	7170118.07	22642294.08
	100	15925134.31	8153226.66	23691232.79
	250	17918652.62	10037571.08	25795627.01
	500	19931755.65	11494898.87	28362923.38
SSP5-8.5 (2050)	5	5373804.84	1624413.53	9121618.42
	10	6306319.35	2182759.42	10430410.34
	25	8034955.56	3085334.72	12982081.79
	50	9085562.92	3840361.41	14328580.05
	100	10667351.16	4978438.84	16350333.49
	250	13076123.02	6728566.41	19415430.88
	500	14330830.26	7971473.69	20682985.98

Projections	ARI	Building loss (USD 2012)		
		Mean fragility function	Storm surge fragility function	Tsunami fragility function
SSP5-8.5 (2100)	5	17664563.10	9018201.55	26302610.96
	10	20023068.83	10630330.00	29407783.24
	25	21915195.98	12251301.41	31569907.36
	50	23855530.39	1382412765	33877974.33
	100	25791017.39	15076751.89	36490941.40
	250	27212364.20	15864113.06	38549840.54
	500	30418422.28	17663724.22	43163131.43

Annex 10: Nauru's annual expected damage per district

Districts	Projections	Annual expected building damage (USD 2012)		
		Mean fragility function	Storm surge fragility function	Tsunami fragility function
Aiwo	Present	91.49	7.88	174.51
	SSP1-1.9 (2050)	491.68	44.11	939.44
	SSP1-1.9 (2100)	2103.63	215.30	4007.92
	SSP5-8.5 (2050)	574.44	53.36	1095.07
	SSP5-8.5 (2100)	12114.57	1455.98	22760.07
Anabar	Present	446181.35	156766.22	735437.96
	SSP1-1.9 (2050)	671042.78	317025.49	1024734.50
	SSP1-1.9 (2100)	1251543.69	715767.42	1786737.93
	SSP5-8.5 (2050)	741687.14	361346.43	1122014.29
	SSP5-8.5 (2100)	1920976.26	1323660.21	2517200.35
Anetan	Present	192586.00	71495.63	313788.84
	SSP1-1.9 (2050)	301320.29	135203.31	467322.48
	SSP1-1.9 (2100)	496157.94	257768.60	734085.47
	SSP5-8.5 (2050)	324894.04	151507.06	498333.26
	SSP5-8.5 (2100)	809305.97	462308.02	1155776.20
Anibare	Present	81027.85	9317.76	152809.79
	SSP1-1.9 (2050)	184278.81	31034.10	337166.08
	SSP1-1.9 (2100)	300624.06	82495.52	518459.66
	SSP5-8.5 (2050)	206524.87	39860.57	372823.48
	SSP5-8.5 (2100)	476841.78	242352.65	711109.72
Baitsi	Present	3682.08	833.05	6518.48
	SSP1-1.9 (2050)	7393.36	2283.23	12508.73
	SSP1-1.9 (2100)	18639.33	7416.47	29868.25
	SSP5-8.5 (2050)	10225.56	3120.10	17346.05
	SSP5-8.5 (2100)	55238.40	28355.07	82060.74

Districts	Projections	Annual expected building damage (USD 2012)		
		Mean fragility function	Storm surge fragility function	Tsunami fragility function
Boe	Present	17177.64	1525.40	32783.83
	SSP1-1.9 (2050)	24836.73	2848.85	46821.86
	SSP1-1.9 (2100)	54740.54	8951.32	100480.40
	SSP5-8.5 (2050)	28560.01	3588.01	53486.19
	SSP5-8.5 (2100)	128892.82	31613.87	226202.08
Ewa	Present	169862.53	33992.27	305825.78
	SSP1-1.9 (2050)	297051.16	78491.22	515844.26
	SSP1-1.9 (2100)	497346.80	196960.51	797495.94
	SSP5-8.5 (2050)	323025.73	89519.23	556640.28
	SSP5-8.5 (2100)	811524.66	482096.38	1140472.87
Ijuw	Present	16497.44	2001.30	30967.63
	SSP1-1.9 (2050)	44388.04	7773.21	81049.85
	SSP1-1.9 (2100)	83374.62	18127.54	148680.73
	SSP5-8.5 (2050)	49720.76	8844.61	90674.84
	SSP5-8.5 (2100)	157140.67	49131.70	265076.55
Meneng	Present	300576.68	44465.26	556696.25
	SSP1-1.9 (2050)	541669.22	126744.88	956441.22
	SSP1-1.9 (2100)	1275610.19	388695.47	2162388.95
	SSP5-8.5 (2050)	604749.25	150170.67	1059156.61
	SSP5-8.5 (2100)	2419476.82	1070804.85	3767253.25
Nibok	Present	51.31	3.61	98.29
	SSP1-1.9 (2050)	142.57	11.41	274.66
	SSP1-1.9 (2100)	863.76	68.38	1660.84
	SSP5-8.5 (2050)	154.91	12.30	298.29
	SSP5-8.5 (2100)	14136.09	1212.00	26942.52
Uaboe	Present	4443.71	536.36	8344.20
	SSP1-1.9 (2050)	12970.43	1809.94	24107.90
	SSP1-1.9 (2100)	31564.74	7196.80	55976.65
	SSP5-8.5 (2050)	18089.27	2500.88	33617.44
	SSP5-8.5 (2100)	88529.17	31989.42	145030.98

Districts	Projections	Annual expected building damage (USD 2012)		
		Mean fragility function	Storm surge fragility function	Tsunami fragility function
Yaren	Present	44228.65	8347.07	80087.08
	SSP1-1.9 (2050)	85537.12	22193.09	148802.21
	SSP1-1.9 (2100)	139445.48	53795.55	225038.21
	SSP5-8.5 (2050)	87936.07	25497.65	150264.82
	SSP5-8.5 (2100)	422357.22	157779.18	687206.03
TOTAL	Present	1276406.71	329291.80	2223532.62
	SSP1-1.9 (2050)	2171122.19	725462.84	3616013.21
	SSP1-1.9 (2100)	4152014.76	1737458.89	6564880.95
	SSP5-8.5 (2050)	2396142.05	836020.87	3955750.62
	SSP5-8.5 (2100)	7316534.42	3882759.34	10747091.34

Produced by the Pacific Community (SPC)
Pacific Community
Private mail bag, Suva, Fiji

Telephone: +679 337 0733
Email: spc@spc.int
Website: www.spc.int

ISBN 978-982-00-1489-3